IMPROVEMENT IN BARRIER PROPERTIES OF POLYMERS USED IN PACKAGING INDUSTRY – PET/N-MXD6 BLENDS

by
GÜLAY BOZOKLU

Submitted to the Graduate School of Engineering and Natural Sciences
In partial fulfillment of the requirements for the degree of
Master of Science

Sabancı University
Spring 2008

IMPROVEMENT IN BARRIER PROPERTIES OF POLYMERS USED IN PACKAGING INDUSTRY – PET/N-MXD6 BLENDS

APPROVED BY

Prof. Dr. Yusuf Menceloğlu .....
(Thesis Supervisor)

Dr. İlhan Özen .....
(Co-Advisor)

Dr. George Robert Wagner .....

Assoc. Prof. Dr. Mehmet Ali Gülgün .....

Asst. Prof. Dr. Melih Papila .....

DATE OF APPROVAL:

IMPROVEMENT IN BARRIER PROPERTIES OF POLYMERS USED IN PACKAGING INDUSTRY – PET/N-MXD6 BLENDS

Gülay BOZOKLU

MAT, MSc. Thesis, 2008

Thesis Supervisor: Prof. Dr. Yusuf Z. MENCELOĞLU

Keywords: oxygen gas permeability, compatibility, blends, poly (m-xylene adipamide), poly (ethylene terephthalate).

ABSTRACT

Traditional packaging materials like glass and metal are increasingly replaced by plastics due to several advantages of plastics which are low density, less energy consumption, ease of processing, weight reduction and cost savings. Unfortunately plastics are permeable to gases while glass and metal are absolute barrier materials. Permeability is an important issue in packaging that relates to product quality and a reasonable shelf life.

Improvement in barrier properties of polyester/polyamide blends used in packaging industry is the main objective of the present study. For this purpose polyethylene terephthalate (PET)/ poly (m-xylene adipamide) (Nylon-MXD6) (95/5 w/w) and PET-co-10I (polyethylene terephthalate-co-isophtahalate random copolymer containing 10 wt. % isophthalic acid (IPA)) / N-MXD6 (95/5 w/w) blends have been prepared with different compatibilizer types and combinations by using a co-rotating intermeshing twin screw extruder. The effects of biaxial orientation, crystallinity, morphology (tortuous pathway), and chemistry on oxygen gas permeability were analyzed by using different characterization techniques like scanning electron microscopy (SEM), differential scanning calorimetry (DSC), spectral-birefringence, and gas permeability analyzer.

The morphological analysis revealed that PET copolymer that consists of 5% sodium sulfonated isophthalate (PET-co-5SIPA) was an effective compatibilizer for both PET/N-MXD6 and PET-co-10I/N-MXD6 blends. Spectral-birefringence technique and DSC analysis were used to understand the crystallization behaviour of the blends. Morphological analysis of films after biaxial stretching indicated that the spherical nylon phase was converted to 75 nm thick ellipsoids during stretching (aspect ratio L/W=6) that creates tortuous pathway for oxygen ingress. PET-co-10I films had low permeability before biaxial stretching compared to unoriented PET films. Stretching ameliorated barrier properties of PET/N-MXD6 films but increased the permeability of PET-co-10I/N-MXD6 blends.

AMBALAJ SANAYİNDE KULLANILAN POLİMERLERİN BARİYER ÖZELLİKLERİNİN İYİLEŞTİRİLMESİ – PET/N-MXD6 KARIŞIMLARI

Gülay BOZOKLU

MAT, Yüksek Lisans Tezi, 2008

Tez Danışmanı: Prof. Dr.Yusuf Z. MENCELOĞLU

Anahtar Kelimeler: oksijen gaz geçirgenliği, uyumluluk, polimer karışımları, poli (m-ksilen adipamid), poli (etilen terefitalat).

ÖZET

Düşük yoğunluk ve enerji tüketimi, üretim kolaylığı, hafiflik, ve maliyet kazanımları gibi bazı avantajlara sahip olan plastikler artan bir şekilde geleneksel ambalaj malzemeleri olan cam ve metalin yerini almaktadır. Cam ve metal mutlak bariyer malzemeleri olmalarına rağmen, plastikler gaz geçirgendirler. Geçirgenlik, ürün kalitesi ve raf ömrününü belirlemesi açısından ambalajlar için hayati önem taşımaktadır.

Bu nedenle bu çalışmanın temel amacı ambalaj endüstrisinde kullanılan poliester/poliamid karışımlarının bariyer özelliklerini iyileştirmektir. Bu amaçla çift burgu ekstrüder kullanılarak farklı uyumlaştırıcı tipleri ve kombinasyonları ile polietilen terefitalat (PET)/poly (m-ksilen adipamid) Naylon-MXD6 (95/5 wt. %) ve 10 wt.% isofitalik asit içeren PET kopolimeri (PET-co-10I)/Naylon-MXD6 karışımları hazırlanmıştır. Taramalı elektron mikroskobu (SEM), diferansiyel taramalı kalorimetre (DSC), spektral çift kırılım, ve gaz geçirgenlik testleri gibi farklı karakterizasyon teknikleri kullanılarak çift yönlü yönelim, kristallinite, morfoloji (dolambaçlı yol), ve kimyanın gaz geçirgenliği üzerindeki etkileri analiz edilmiştir.

SEM imajlarında gözlenen dispers faz boyutundaki azalma % 5 sodyum sulfonlanmış isofitalat içeren PET kopolimerinin (PET-co-5SIPA'nın) PET/N-MXD6 ve PET-co-10I/N-MXD6 karışımlarında uyumlaştırı olarak etkinliğini göstermektedir. Spektral çift kırılım ve DSC analizleri karışımların kristallenme davranışını anlamak için kullanılmıştır. Çift yönlü gerdirme sonrasındaki morfolojik analizler küresel naylon fazın gerdirme sırasında modifiye edilerek ortalama 75 nm kalınlığında elipsler (en/boy oranı=6) haline dönüştüğünü ve bunun oksijen girişi için dolambaçlı bir yol yarattığını göstermiştir. PET filmlerine kıyasla PET-co-10I filmleri çift yönlü gerdirme öncesinde daha düşük geçirgenlik değerlerine sahiptir. Gerdirme PET/N-MXD6 filmlerinin bariyer özelliklerini iyileştirirken, PET-co-10I/N-MXD6 karışımlarının geçirgenlik değerlerini yükseltmiştir.

To my parents…

Gülseren & Suat Bozoklu

ACKNOWLEDGEMENTS

First of all, I would like to express my special thanks to my thesis supervisor Prof. Dr. Yusuf Z. Menceloğlu for his advises and support in this thesis. His positive attitude and practical approach will be a model for all my life and future studies. I am very grateful to my co-advisor Dr. İlhan Özen who has shared his knowledge and experience with me during this thesis. I would like to give sincere gratitude to Dr. George R. Wagner for his critical thinking and endless desire to share his ideas on the subject. I am also very thankful to all faculty members in Material Science Program who are Cleva Ow-Yang, Alpay Taralp, Canan Atılgan, Melih Papila and Yuda Yürüm.

I specially thank to Assoc. Prof. Dr. Mehmet Ali Gülgün for being a guide for me during my studies starting from my freshman year. Without his support and encouragement I would not go this further. He is the one that "thank you" is not enough to tell.

I would like to thank TUBITAK for financial support. I also would like to thank I2CAM (Institute for Complex Adaptive Matter) for providing me funding to travel USA for my experiments.

I would like to thank Prof. Dr. Mükerrem Çakmak and his group for their kindness and help on biaxial orientation and characterization, Atilla Alkan from Brisa for his help in SEM sample preparation, Engin Küçükaltın from Advansa for his kind help, Mehmet Manyas in IC for his positivity and helps for finding resources, Mehmet Güler for his endless motivation to machine anything that I needed through this project.

I kindly thank Cahit Dalgıçdır for helping me with my experiments and for his friendship. My special thanks are for my friends and colleagues, without them my master studies would not be that much fun, Emre Fırlar, Özge Malay, Çınar Öncel, Seren Yüksel, Firuze Okyay, Vanya Uluç, Funda İnceoğlu, Eren Şimşek, Gökhan Kaçar, Burcu Saner, İbrahim İnanç.

Finally, I would like to thank my parents. Their endless love, understanding and support were the main motivation of this study. Therefore this thesis is dedicated to them.

TABLE OF CONTENTS

LIST OF FIGURES

LIST OF TABLES

LIST OF ABBREVIATIONS

PET:	Polyethylene terephthalate
PET-co-10I:	PET copolymer containing 10% IPA
N-MXD6:	Poly (m-xylene adipamide)
EVOH:	Ethylene vinyl alcohol
PP:	Polypropylene
PE:	Polyethylene
PS:	Polystyrene
PC:	Polycarbonate
PVC:	Polyvinyl chloride
SEM:	Scanning Electron Microscopy
DSC:	Differential Scanning Calorimetry
TGA:	Thermo gravimetric Analysis
Tg:	Glass transition temperature
Tm:	Melting temperature
Tcc:	Cold crystallization temperature
PVD:	Physical vapor deposition
PECVD:	Plasma-enhanced chemical vapor deposition
LCP:	Liquid crystalline polymers
IPA:	Isophthalic acid
TPA:	Terephthalic acid
SIC:	Strain- induced crystallization
GTR:	Gas transmission rate
OTR:	Oxygen transmission rate
WVTR:	Water vapor transmission rate
RI:	Refractive index

LIST OF NOTATIONS USED FOR BLENDS

Notation	Sample	Wt %
PET		
EP100	PET/N-MXD6	95/5
EP101	PET/N-MXD6/PET-co-5SIPA/CoAc	85.5/5/9.5/250ppm
EP102	PET/ N-MXD6/CTPB/CoAc	94/5/1/250ppm
EP103	PET/ N-MXD6/CTPB/PET-co-5SIPA/CoAc	84.5/5/1/9.5/250ppm
EP104	PET/ N-MXD6/CTPB+HTPB(1/2)/CoAc	94/5/1/250ppm
EP105	PET/N-MXD6/CTPB+HTPB(1/2)/PET-co-5SIPA/CoAc	84.5/5/1/9.5/250ppm
PET-co-10I		
EO100	PET-co-10I/N-MXD6	95/5
EO101	PET-co-10I /N-MXD6/PET-co-5SIPA/CoAc	85.5/5/9.5/250ppm
EO102	PET-co-10I/N-MXD6/CTPB/CoAc	94/5/1/250ppm
EO103	PET-co-10I/N-MXD6/CTPB/PET-co-5SIPA/CoAc	84.5/5/1/9.5/250ppm
EO104	PET-co-10I/N-MXD6/CTPB+HTPB(1/2)/CoAc	94/5/1/250ppm
EO105	PET-co-10I/NMXD6/CTPB+HTPB(1/2)/PET-co-5SIPA/CoAc	84.5/5/1/9.5/250ppm

CHAPTER 1

1. INTRODUCTION

Plastics in packaging provide reduction in weight due to their low density which results in less energy consumption combined with the lower melting temperatures as compared to glass and metal, which makes them easy to process and manufacture [1]. The growth of plastics packaging started in 1970s and reached a considerably high ratio in plastics market; currently packaging occupies 38 % of plastics market [2]. Polymers used most commonly in packaging are polyolefins (PP, PE), polystyrene, polyvinyl chloride, and polyethylene terephthalate (PET).

Polyethylene terephthalate (PET) is a linear, semi crystalline thermoplastic resin of polyester family that is widely used for food packaging applications. Advantages of PET are its high optical clarity, high mechanical strength, low cost, low permeability to oxygen and carbon dioxide, and dimensional stability during filling. Largest use of polyester is in textile fibers. However, packaging has been a growing use of PET. In 2002, 42 % share of soft drink packaging and 5 % of beer market is expected to be holding by PET [1].

Studies on improvement of barrier properties are currently focused on blending with high barrier polymers like ethylene vinyl alcohol copolymer (EVOH) and polyamides. EVOH has excellent gas barrier properties; however it is weak against moisture [3]. Nylons, which are aromatic polyamides, are much less moisture sensitive compared to EVOH. Thus, nylons show greater gas barrier than EVOH in humid atmospheres. They are also favored more in PET blends since their melting temperature is close to PET [4].

Nylons are linear thermoplastic polyamides that find usage in textile as fibers mostly. They are clear, thermoformable, strong and have good chemical resistance and high barrier against gases and aromas. In packaging applications, nylons are mostly used as middle layer in multilayer structure or as single film.

Films	Molecular structure
N-MXD6	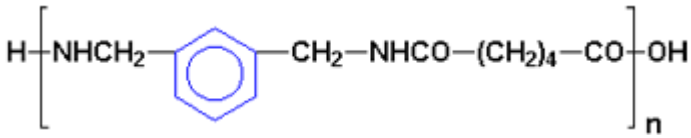
Nylon 6	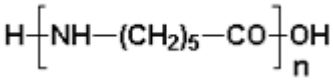
Nylon 6,6	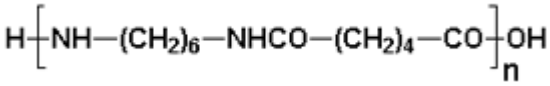

Table 1.1- Molecular structures of Nylons and PET [5].

A special nylon called poly (m-xylene adipamide) (Nylon-MXD6) has attracted researchers interest due to its barrier properties being higher than EVOH (ethylene vinyl alcohol) at humid atmospheres. The molecular structure of N-MXD6 is given in Table 1.1 in comparison to nylon 6 and nylon 6,6. The aromatic ring in the structure decreases flexibility and chain alignment thus hinders crystallization. The rigidity imparted by the ring in the main chain results in better gas barrier and thermal properties than other packaging plastics as given in Table 1.2 at humid atmospheres [6]. MXD6 can also be further activated against oxygen transport by incorporating a transition metal oxidation catalyst, such as Co(II), that then converts the polyamide into a sacrificial oxygen scavenger [7].

Films	Oxygen permeation rate (cc/m2.day.atm) 20 µ, 23°C		
	60 % RH	80 % RH	90 % RH
N-MXD6 (oriented)	2,8	3,5	5,5
N-MXD6 (unoriented)	4,3	7,5	20
EVOH-32	0,5	4,5	50
EVOH-44	2	8,5	43
Nylon 6	40	52	90
PET(oriented)	80	80	80

Table 1.2- Oxygen permeation rate of films at various moisture levels [5].

The studies on enhancement of the barrier properties of polymers could only succeed with comprehensive analysis and understanding of the relationships between structure, processing and final properties. Therefore in this section background of gas permeation, polymer structural factors and processing will be explained briefly.

1.1. Gas Permeation in Polymeric Materials

An ideal barrier material for packaging is the one that does not interact with product and the environment. The main function of a package is to hold and protect the product. Even small oxygen ingress or the escape of carbon dioxide or aromas from the product deteriorates the taste of packaged food products. Especially for carbonated beverages the main problem is the permeation of oxygen and carbon dioxide; therefore packaging systems that provide high barrier must be designed in order to keep the beverage appetizing. Metal and glass are absolute barriers to gases. On the other hand polymers are permeable to gases through their molecular cavities or microvoids as shown in Figure 1.1.

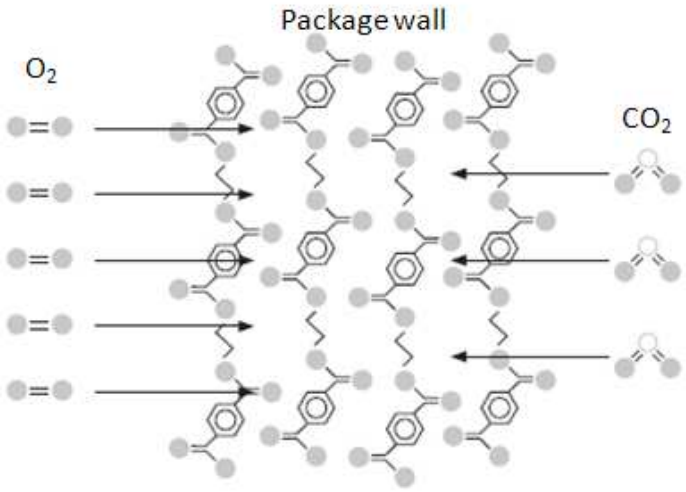

Figure 1.1- Gas permeability through a plastic package wall [8].

Permeation refers to the transport of matter through a package wall. Penetrate transport in polymers are explained with the activated diffusion mechanism [9] in which gas dissolved in the film at one surface, then migrates through the film and then desorbs into the food product (Figure 1.2). Therefore the total permeation process consists of sorption, Fickian diffusion and desorption.

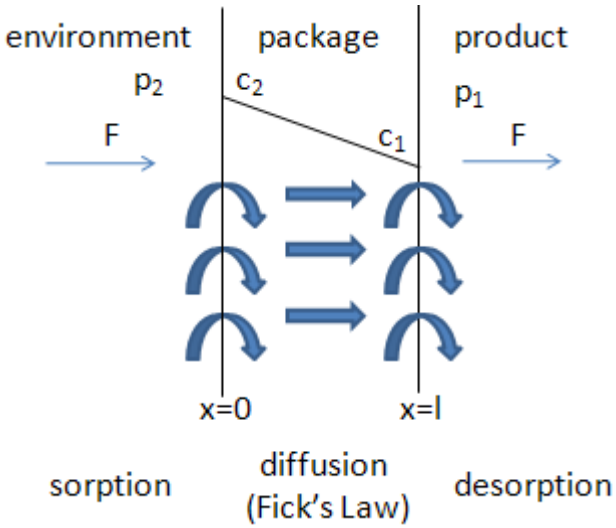

Figure 1.2- Interactions between permeant gas and plastic package.

Free volume is an important concept in transport phenomena used to explain the transport properties. Free volume refers to the microcavities inside the polymer and permeant molecules diffuse through these cavities. Number and size of cavities determine the transport properties of a permeant inside the polymer. Permeability is a function of both solubility and diffusivity (P=D*S). Solubility is proportional to amount of free volume, where oxygen sorption is the process of filling free volume holes by oxygen. Permeant gas diffuses through free volume inside the plastic package which are dynamic holes created by thermally activated conformational changes and segmental motions. Derivation of permeability coefficient P from application of Fick's law of diffusivity and Henry's law of solubility is given in Appendix A. Resistance of polymers to diffusion and sorption of molecules determines their barrier properties.

1.1.1. Experimental Determination of Permeability

There exist two different test methods to determine oxygen permeability of packaging samples: differential pressure method and equal pressure method [10]. Permeation cavity is divided into two independent parts by sample package in the form of film or bottle. In differential pressure method one side is filled with test gas of 1 atm while the other side is kept at vacuum. Test gas migrates through the film into low-pressure side, and causes a pressure change which is detected with a high precision vacuum gauge and used to calculate the gas transmission rate (GTR).

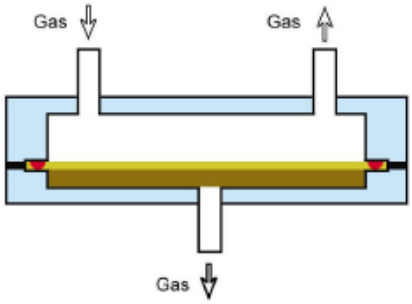

Figure 1.3- Test principle of the differential pressure method [10].

In equal pressure method on one side testing gas (oxygen) flows and on the other side dry carrier gas (nitrogen) flows. Pressure of the two sides is equal but oxygen partial pressure is different. Oxygen transmits through the film and carried to the sensor by nitrogen. Sensor measures the oxygen permeance in nitrogen carrier gas and provides the oxygen transmission rate (OTR). However, its application is not as wide as differential-pressure method. The calculation of GTR and OTR is given in Appendix B.

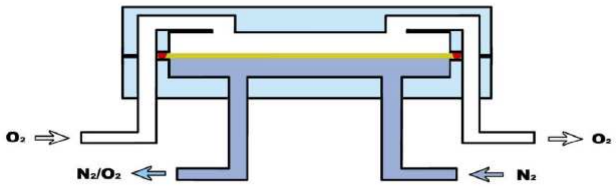

Figure 1.4- Test principle of the equal pressure method [10].

The units of gas transmission rate are also different from each other where the unit of differential pressure method is cm^3/m^2.24h.1atm and the unit of equal pressure method is cm^3/m^2.24h. There is no comparability between the two methods. Permeability is obtained by multiplying gas transmission rate with thickness of the film or bottle. 29 different units for permeability coefficient exist in the literature which makes it hard to make comparisons [11]. Therefore standardization of permeability testing is highly required. In this thesis equal pressure method is used, therefore the units of permeability coefficient will be in ml.cm/m^2.day, OTR and WVTR values of the films will be given in Appendix C.

The most common method used to measure water vapor permeability is the gravimetric method also called cup method [12]. The specimen that is sealed inside the cup is put in constant temperature and humidity atmosphere. Water vapor permeability is

calculated with the measured weight decrease of the cup. The units are given in g.cm/m^2.day.

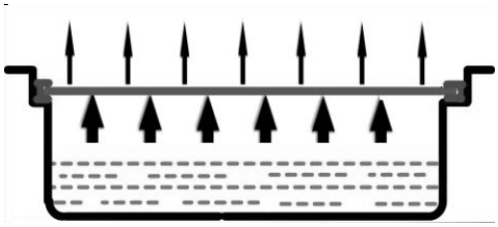

Figure 1.5- Test principle of the gravimetric cup method [12].

1.1.2. Variables affecting Permeability

Permeation of low molecular weight substances depends on both solubility and the diffusion of the molecules as shown in Figure 1.2. In order to obtain low permeability, both solubility and diffusion should be decreased. Polymer chemistry, morphology, crystallinity and orientation are important factors determining barrier properties of the polymers.

1.1.2.1. Chemistry

Chemistry is the main factor determining the barrier properties. Chemical compositions, polarity, stiffness of the polymer chain, bulkiness of side and backbone-chain groups significantly affect barrier properties of the polymers. The affinity between a permeant and the polymer is determined by the chemistry. Low solubility of permeant due to chemical difference with the polymer matrix results in low permeability since permeability is related to both solubility and diffusion. Cohesive energy density is a parameter affecting permeability of polymers for low molecular weight substances. It gives information about the strength of the interaction between the molecules and is used to explain the effect of different chemical groups on permeability of a polymer. By changing functional groups it is possible to alter the barrier properties of the polymers as shown in Figure 1.6 for polyethylene. Incorporation of voluminous groups can either enhance or disrupt barrier properties by providing high or low intermolecular cohesion. In general small chemical groups decrease oxygen permeability by increasing the necessary intermolecular cohesion as –H, -O, -CN of Figure 1.6. On the other hand introduction of apolar voluminous groups could increase permeability by creating large free volume as $-CH_2C_3H_7$ or could decrease permeability by increasing cohesive energy density as $–COOCH_3$ as shown in Figure 1.6.

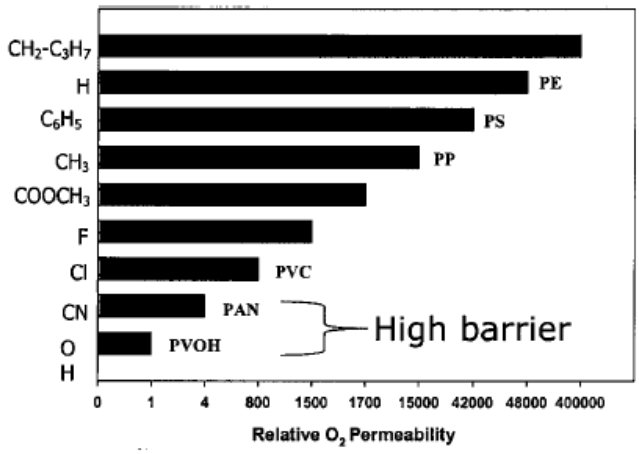

Figure 1.6- Effect of different pendant groups on oxygen permeability [13].

1.1.2.1.1. PET Copolymers

Chemical modification by copolymerization of PET has significant attraction to industry and academia. Typical co-monomers incorporated into the chemical backbone of PET for packaging applications include 1,4-cyclohexanedimethanol, diethylene glycol, and especially isophthalic acid (IPA) [14].

PETG is a glycol modified PET copolymer which is produced by the addition of cyclohexane dimethanol instead of ethylene glycol into the polymerization. Cyclohexane dimethanol hinders crystallization and lowers melting temperature of the polymer. PETG has high stiffness, good toughness at low temperatures and better melt strength than PET. PETG is amorphous, clear and colorless co-polyester that has a wide application area in packaging.

Poly (ethylene isophthalate) which is a structural isomer of PET has the same chemical structure as PET except its carbonyl groups are attached in the 1,3 meta positions of its phenyl rings instead of the 1,4-para positions as shown in Figure 1.8. Studies on modifying PET by incorporating isophthalic acid that decrease linearity and crystallization rate showed that PET with isophthalic acid has higher barrier properties than PET [14-20]. Permeability is reported to decrease from 0,424 for PET to 0,371 for PET-b-10I (PET containing 10% isophthalic acid) and further to 0,278 cm^3 (STP) cm m^{-2} atm^{-1} day $^{-1}$ for PET-b-20I (PET containing 20% isophthalic acid) [19]. Kotek et al. explained the reason for reduction of permeability by the reduction in flipping of the rings in PET structure with

the addition of isophthalic acid. Attachment of carbonyl groups to the phenyl ring in 1,4 para positions provides linearity and allows flipping of the rings in PET. The flipping of phenyl rings may allow gases to permeate through, with the flipping phenyl rings acting much like a trap door and valve [21]. Therefore reduction in permeability with the addition of isophthalic acid is attributed to the nonlinear attachment of phenyl rings in isophthalic acid, which does not allow flipping of the phenyl rings.

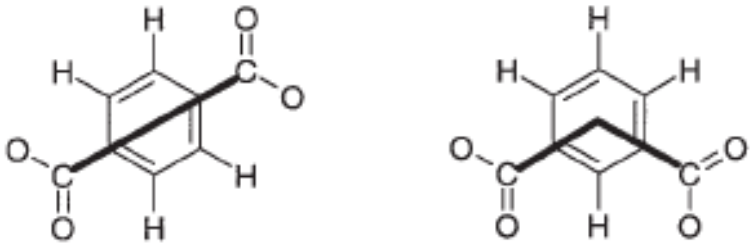

Figure 1.7- The attachment of carbonyl groups to the phenyl rings in PET (with 1,4-(para-) linked terephthalic acid) and PEI (with 1,3-(*meta*-) linked isophthalic acid) [21].

1.1.2.2. Polymer Morphology

The lowest energy state (the lowest Gibbs free energy) that a polymer can obtain by arranging its chains is a crystal form. The factors determining the morphology of a polymer are chemical composition, degree of polymerization, chain conformation, molecular architecture, thermo mechanical history and processing conditions. Plastics used in packaging are mostly semi-crystalline materials containing both conformationally ordered crystalline fraction and amorphous parts without any conformational regularity. The assumption taken during calculation of permeability, sorption and diffusion for polymers is that they just contain homogenous, isotropic amorphous phase. However, the polymers in reality consist of crystalline phase which makes permeation be a complex phenomenon. Crystalline phase decreases the sorption by excluding large molecules like CO_2 or O_2 with close atomic packing creating high density regions. Therefore gases and vapors can just be absorbed through amorphous regions. The dispersed crystalline regions inside the polymer create a tortuous pathway for the diffusion and decrease diffusion rate. Crystalline parts are impermeable to the permeation of low molecular weight substances, which makes amorphous sides the only pathway for the permeation. Therefore permeant molecules have

to go through the crystalline sides and reach to the amorphous area to be able to enter inside the package as shown in Figure 1.8.

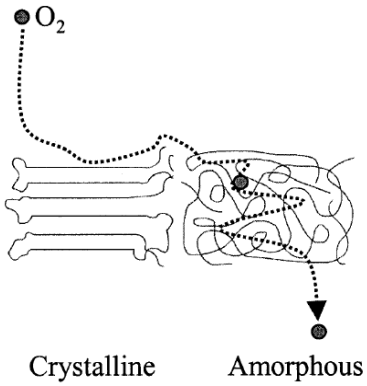

Figure 1.8-Migration of oxygen in a semi-crystalline polymer [13].

Polymers with symmetrical unsaturated monomers (like PE and PVC) crystallize easily; on the other hand asymmetrical polymers like PP crystallize only in some isomeric conditions like syndiotactic or isotactic. Atactic polymers with asymmetric monomers can crystallize if the substituents are small and polar like in EVOH and PAN. In contrast, if the side groups are too bulky the polymer cannot crystallize like in PS. Step-reaction polymers, produced by bifunctional monomers containing alcohol, acid and amine can crystallize. The bifunctionality in these polymers forcing the chain growth only in one direction results in highly ordered chains like in nylon 6 and nylon 6, 6. Polymers containing aromatic or cyclohexane rings are crystallizable if the substitutions are in 1, 4 positions like in PET and PC. Other substitutions like 1, 3 hinders crystallization by increasing randomness [1].

Degree of crystallinity of a polymer is basically the ratio of the crystalline part to the amorphous part. The main method to determine the degree of crystallinity is x-ray scattering which is not used extensively since it is expensive and complex. Another method is the density gradient method (ASTM D 1505). The crystallinity is determined from the position of the plastic beads in the density gradient column compared to the calibrated glass beads of known density. Crystallinity of the polymers are mostly determined by using Differential Scanning Calorimetry (DSC) by adapting Equation 1.1 in which the effect of cold crystallization peak is removed from the melting peak in order to determine the percent crystallinity in the polymer. Enthalpy given in the denominator of the Equation 1.1 is a theoretical value for the peak area of the melt if it would be 100% crystalline. The enthalpy for 100% crystalline PET is 140 J/g [22].

$$Crystallinity\% = 100 * \frac{abs(PeakArea(melt) + PeakArea(ColdCryst.)}{Enthalphy(Melt,100\%Crystallinity)} \quad (1.1)$$

1.1.2.3. Polymer Orientation

Fabrication of polyester food packages is mostly accompanied by orientation. Amorphous PET has low mechanical properties, low transport properties, low dimensional stability and high extensibility, thus it has little commercial interest [6]. The mechanical and transport properties of PET are enhanced by orientation. Fabrication methods for PET packaging involve injection, reheat-stretch and extrusion blow molding in which orientation has an important role. Different modes of stretching are shown in Figure 1.9. Uniaxial or biaxial drawing leads to strain-induced crystallized regions, orientation of the chains and densification (reduction in free volume) in pure PET or blends, which decreases permeability and increases strength of the material in the direction of stretch. Starting from 80s, extensive studies are carried out in order to understand the relationships between orientation, crystallinity, permeability and mechanical properties of PET [23-30]. The results revealed that stretching of polymeric films decreases permeability and increases mechanical properties due to stress induced crystallization and orientation of the chains.

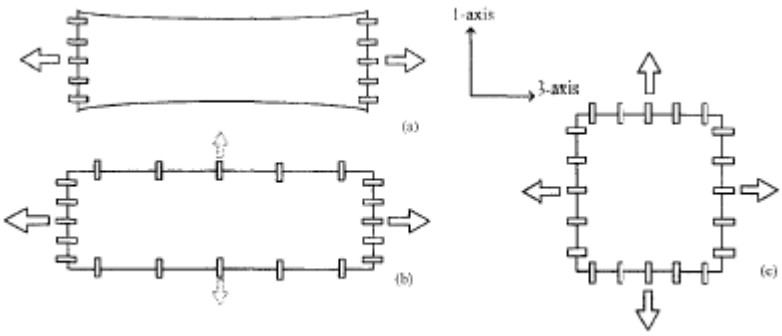

Figure 1.9- Stretching modes: (a)uniaxial, (b)uniaxial constant width, (c)biaxial drawing [31].

Polymer films or sheets are oriented above Tg in response to external stress. Films used in packaging could be unoriented, uniaxially oriented, or biaxially oriented. Orientation results into an ordered structure which increases crystallinity, alignment of

chains, and densification of amorphous phase by decreasing free volume. As shown in Figure 1.10 unoriented cast films have a crystallinity of 0-5 %, whereas uni-axially stretched films have a crystallinity of 10 to 20 %. Bi-axially stretched films have a 30-40 % crystallinity ratio which could be raised to 50 % after heat setting.

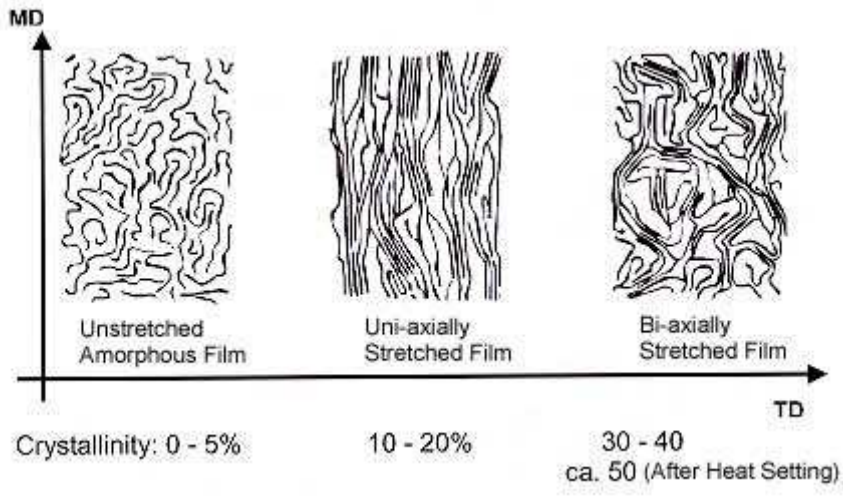

Figure 1.10- Percent crystallinity before and after stretching [32].

Orientation is also used to modify the morphologies of the dispersed phase in polymer blending in order to decrease permeability. The barrier properties of a final blend depend not only on the composition or the intrinsic barrier properties of the components but also on the final morphology of the blend [33]. Spherical morphology of high barrier dispersed phase only gives moderate permeability, however laminar morphology dramatically decreases the permeability [4, 33-37]. The transformation of spheres into high aspect ratio platelets creates a tortuous pathway for the diffusion of low molecular weight molecules and thus decreases the permeability. As shown in Figure 1.11 after orientation spherical morphology is transformed into laminar morphology which increases the path length that oxygen travels. Tortuosity factor, "$\tau=d'/d$" which is the ratio of the distance travelled by the oxygen to the thickness of the film is an important parameter determining the permeability.

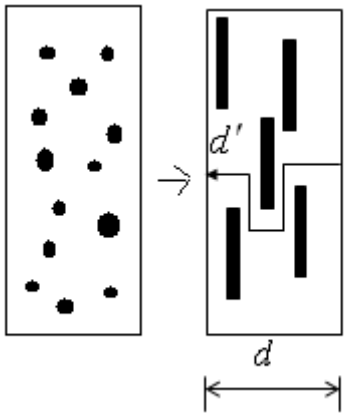

Figure 1.11- Morphology of a blend before and after orientation**.**

Nature of stress strain curves that are recorded during the process of stretching is widely studied by different researchers. Figure 1.12 shows typical plastic behavior for PET. As the specimen is stretched the load rises rapidly at first (A), up to yield point (B). With further elongation, the curve shows a plateau where the load stays at a constant level while large deformations are accomplished (C). After this, stress strain curve shows an upswing which indicates the onset of strain hardening. The extension ratio at the onset of strain hardening is called as natural draw ratio (D). The alignment of polymer chains results in high degree of deformation which leads to strain-induced crystallization (E). Orientation is quite important for plastics processing. It is required to work above natural draw ratio in order to obtain thinner, uniform and less expensive products. Therefore knowledge of strain hardening for the polymers used is important in determining extension ratios required to achieve uniformity of wall thickness and properties in the final product [38].

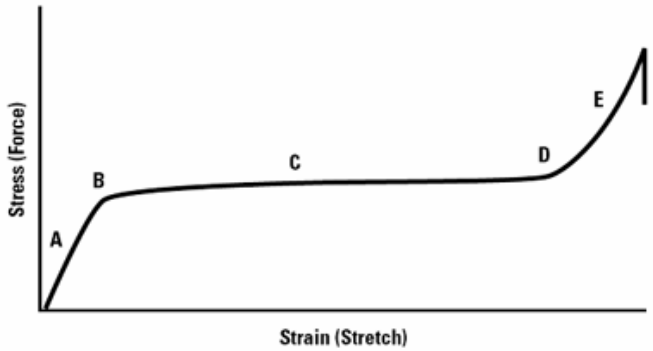

Figure 1.12- Typical plastic behavior for PET [39].

In order to visualize orientation and crystallinity in polymers, various methods are developed like birefringence, retardation techniques, dichroism, and x-ray diffraction [40]. Birefringence measurement is the most common method to evaluate both orientation and relaxation phenomena of polymers. Birefringence is due to a difference between principal refractive indices within a material and its variations that are related to the orientation of macromolecules. The refractive index represents the slowing of progress of an electromagnetic wave through a material because of interaction of the wave with polarizable molecules [40]. During stretching by the formation of crystallites optical symmetry changes and this could be observed with a spectral birefringence stretching machine in order to understand effects of orientation on the polymer.

1.1.2.4. Polymer Plasticization

Polymer plasticization has detrimental effects on barrier properties which results from losses of intermolecular cohesion and Tg depletion due to chemical interactions between polymer-penetrant molecule and their environment. Most of the high barrier polymers have very low barrier performance to polar solvents like water. For instance relative humidity significantly decreases the barrier properties of EVOH. In contrast, barrier properties of an amorphous polyamide increases with the moisture. This is explained by the fact that moisture is not disrupting the existing hydrogen bonding in polyamide instead bonding to free amide groups, so that free volume is decreasing against oxygen diffusion.

1.2. Barrier Technologies

There are commonly two routes to produce high barrier packages: addition of high barrier material as layered film or incorporation of high barrier material to the polymer used. Traditionally aluminium layer or aluminium coating is used to provide high barrier properties. However in terms of product visibility and transparency, aluminium is not favored. Another disadvantage of aluminium is the high energy consumption during production that makes aluminium an environmentally unfriendly material for packaging applications. Glass in packaging is also losing its popularity because of the tendency to weight reduction, reduced breakage and cost savings [41].

One of the most important requirements for plastics to be used in packaging is good barrier properties like metal and glass. In order for PET to be used in applications that require relatively low permeability, several modifications such as barrier coatings [42-47], new barrier polymers (liquid crystal polymers) [48-51], polymer-clay nanocomposites [52-54], multilayerization [55-57] and blending [3, 4, 33-37, 58-60] are under the spotlight of researchers.

In this section recent barrier technologies like thin coatings, new barrier materials, nanocomposites, multilayerization and blending will be explained briefly.

1.2.1. Thin Coatings

Thing coatings are generally SiO_x films which are developed by physical vapor deposition (PVD) of SiO, or plasma-enhanced chemical vapor deposition (PECVD) of gaseous organosilane and oxygen on PET, PP, or PA (polyamide). SiO_x films result in transparent, water resistant, microwaveable and high barrier packages [47]. Limited flexibility and low crack resistance and high production costs slow down their application in packaging industry. PECVD of hydrocarbons results in similar barrier properties as that of SiO_x films but with better mechanical resistance. Nonetheless, due to high costs; this process has not found usage in industrial applications up to now.

Ormocers, that are inorganic-organic hybrid polymers produced by sol-gel chemistry developed in Fraunhofer Institute in Wurzburg, provide high barrier when used independently or with SiO_x films. Deposition of melamine by PVD also results in thin, transparent, low cost and high barrier films [41]. However since melamine is water soluble, water sensitivity is limiting the usage of these films.

1.2.2. Nanocomposites

Incorporation of inorganic materials with high aspect ratio into polymers results in high barrier nanocomposites. The improvement in barrier properties is provided by the increase in the tortuosity of the diffusion path of the gas. Nanocomposites are mostly transparent since they are filled with small size particles. Different types of clays are used as fillers for polymers. The main difficulty of preparing a nanocomposite is the dispersion of the filler, which is overcome by using compatibilizers that add to the cost of the product.

Nanocomposites research revealed an amelioration of barrier properties by a factor of 2-20, when using 1-5% filler [1]. The improvements in dispersion with a reasonable cost addition will extend the usage of nanocomposites in packaging.

1.2.3. New Barrier Polymers

Liquid crystalline polymers (LCP) are being developed to be used as barrier materials in packaging applications. Different companies are in search to find new barrier materials like Dow with a new thermoplastic epoxy resin (polyamino ethers) and P&G with a high barrier biodegradable polymer [41]. However cost of these new materials is too high to be used extensively.

1.2.4. Multilayerization

Currently multilayer extrusion is widely used to produce low permeability plastic packages. In multilayer extrusion, middle layer is occupied by a high barrier material (i.e. EVOH, N-MXD6) whereas the outer layers are less expensive humidity resistive materials (i.e. PE, PP, PET) as shown in Figure 1.13. This production method requires multiple dies and appropriate adhesives between the layers, so that it is both expensive and highly complex method compared to blending [33].

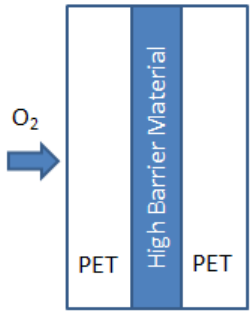

Figure 1.13- Multilayer structure for a high barrier package.

1.2.5. Blends

Blending is an alternative way to produce high barrier materials, in which laminar morphology of the dispersed phase is formed to enhance the barrier properties [35]. Blending provides high barrier properties at a reasonable cost by incorporating a small amount of expensive high barrier material into an inexpensive matrix polymer. The morphology of the blends plays an important role for improving the barrier properties. Figure 1.14 shows the effect of different morphologies on barrier properties. Accordingly the lowest permeability values are obtained at the laminar structure and the highest are observed at particulate system.

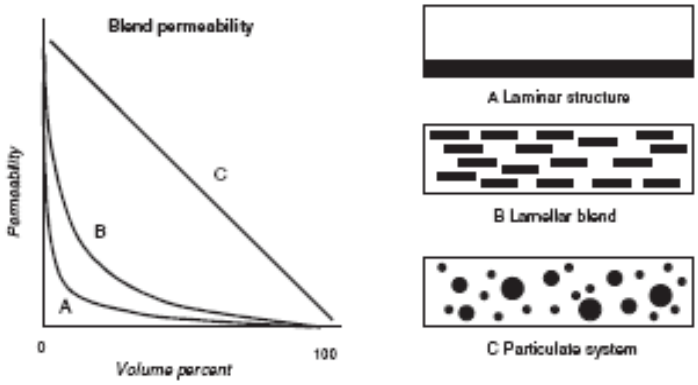

Figure 1.14- Effect of morphology on blend permeability [41].

Comparison of currently available barrier technologies clearly demonstrates that blending is the most effective method that is both cheap and easy to manufacture. Therefore in this study barrier properties of PET are studied to be enhanced by blending with N-MXD6 which is a high barrier material. The incompatibility of polymers in blending requires additional studies of compatibilization in order to obtain low permeability and high strength.

1.2.5.1. Compatibilization

Compatibilization is the most important part of polymer blending where graft or block copolymers are used as interfacial agents in polymer blends. There are a lot of patents related to this issue in recent decades. Interest in understanding the nature of polymer chains near interfaces and surfaces have led to the development of compatibilizers. In order to be effective at the interface, a compatibilizer needs to have chemically different blocks, some

being miscible with one component and some being miscible with the other components of the blend. Compatibilizers are effective in improving blends in several ways. In a first one, it lowers the interfacial tension between the phases, and the second is that the compatibilizer can reduce the agglomeration of domains [61]. Therefore, compatibilizers increase the adhesion between the phases by decreasing the size of the dispersed phase and consequently enhance the mechanical strength of the blends by making it possible to transfer stresses from one phase to another one efficiently.

Both blend morphology and degree of crystallinity depend on efficient stress transfer from matrix phase to the dispersed phase, which could be maintained by modifying interphase of immiscible blends with compatibilizers. Commercial interest in PET/N-MXD6 blends increased the number of studies on compatibilization of these blends. The presence of polar functional groups in PET and N-MXD6 made it possible for the realization of specific interactions between these polymers. Earlier studies pointed out the possibility of compatibilization during melt blending via ester-amide interchange reactions [62], which was not favored due to necessity of catalysts and slow processing times. Immiscible blends are compatibilized generally with the addition of interacting functional groups into blend components. Several types of interactions that have been investigated are: acid-base, hydrogen bonding, charge-transfer complex, ion-dipole, ion-ion, and metal coordination [63, 64]. Ionomers decrease heat of mixing for immiscible blends by forming specific interactions. Previous studies have shown that the use of polyester ionomers gave out reduction in size of the dispersed phase that results from the decrease in interfacial tension due to these specific interactions [34, 37].

1.3. PET Processing

Film casting is widely used to produce PET films. Cast film process involves five steps: feeding, melting, shaping, cooling and winding. The polymer is fed through hopper into the extruder where it is melted and metered. Afterwards melt is shaped through a flat die and passed over cooling rollers while pulled uniaxially to the machine direction. Some cast film machines also have transverse direction stretching as shown in Figure 1.5. Finally the film is rolled on winders.

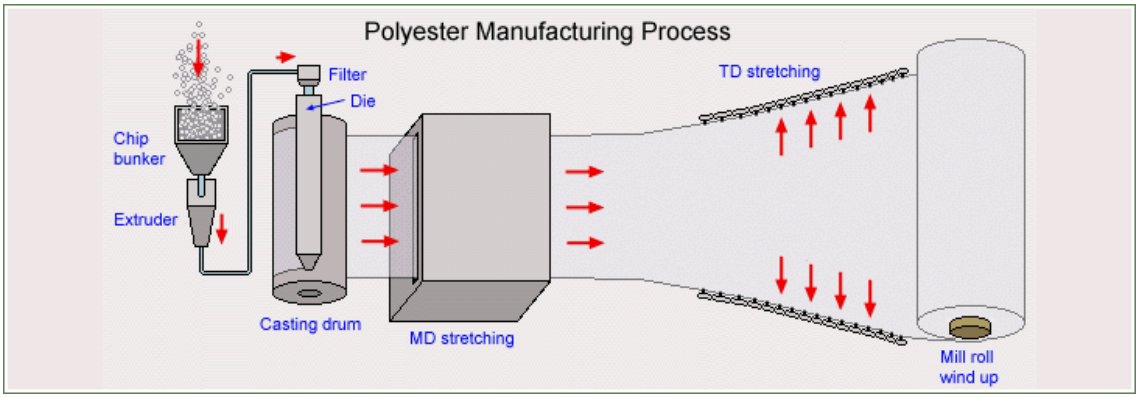

Figure 1.15- Polyester manufacturing process [65].

It is important to control processing parameters in order to obtain products with required properties. Process temperature (extruder unit temperature and chill roller temperature) should be chosen carefully in order to avoid degradation of the polymer. Screw design has to be appropriate for PET. Speed of the line and the screw speed are also crucial determining film thickness and uniformity. The quality of the die is the most crucial point in film casting. Scratches and deformations on the die result in films without smoothness and uniformity in thickness. Cooling speed determines the polymer crystallinity.

It is very well known that even low moisture content causes a hydrolytic degradation when processing PET at high temperatures which impairs mechanical and end use properties. Therefore a proper drying of PET before processing is important. The final moisture content should be less than 0,005% [6] to be able to avoid hydrolytic degradation during processing. In industrial processing, PET is transformed to extruder feed hopper through dehumidifier drier while it is hot.

Intrinsic viscosity (IV) is an important property of PET, with which processing conditions are set and quality of product is determined. IV of a polymer depends on the length of the chains. If the chains are longer, the IV is higher. The length of the chains can be controlled during polymerization. For instance when 100% virgin PET is dried and molded correctly, the pellet-to-preform drop in IV should not exceed approximately 0.03 dl/g [39]. For polyester fiber an IV of 0,60 dl/g, for film 0,65 dl/g, for bottles 0,76-0,84 dl/g, for tire cord 0,85 dl/g is required to have a high quality final product [66]. As shown in Figure 1.16, IV has a drastic effect on mechanical properties. Therefore it is necessary to

find the optimum processing conditions that would end up with acceptable IV values for the product.

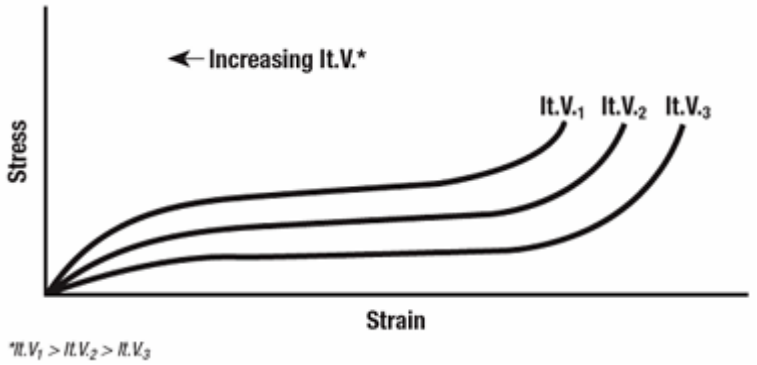

Figure 1.16- Effect of intrinsic viscosity on stress strain curves [39].

1.4. Objective of the study

The objective of this study is to understand the factors affecting barrier properties of polyester/polyamide blends and by doing so improve the barrier properties. The lack of quantitative relationships between thermo mechanical history and the resulting polymer properties are the main obstacle limiting the development of new plastic products. The number of parameters affecting final properties and the complexity of the problem are preventing researchers from reaching a solution. Up to now, very few studies were carried out on N-MXD6. Therefore, an understanding of the relationships between biaxial orientation, crystallinity, morphology (tortuous pathway) and chemistry is not complete yet. This study aims to enhance the knowledge on PET/N-MXD6 blends. For this purpose, PET/ Nylon-MXD6 (95/5 wt.) and (a PET copolymer containing %10 isophthalic acid) PET-co-10I/Nylon-MXD6 (95/5 wt.) blends have been prepared with different compatibilizer types by using a co-rotating intermeshing twin screw extruder that provides high shear necessary in PET processing. The effects of biaxial orientation, crystallinity, morphology (tortuous pathway) and chemistry on gas permeability are analyzed and discussed.

CHAPTER 2

2. EXPERIMENTAL

2.1. Materials

Two different types of PET were used as matrix polymers: Melinar B60® (CSD grade PET, IV: 0,82 dl/g) and OptraH® (IV:0,82 dl/g) which consists of 90 wt.% Terephthalic acid (TPA) and 10 wt.% Isophthalic acid (IPA). Matrix polymers were provided from Artenius UK. Dispersed phase Poly (m-xylene adipamide) (N-MXD6) (Mw: 25,000 g/mole) was provided from Mitsubishi Gas Chemical Company Inc. under the name of Nylon-MXD6 Grade 6007. A copolymer of PET-co-5SIPA which is a product of Artenius UK consists of 5% sodium sulfonated isophthalate was used as compatibilizer for PET blends. Liquid hydroxyl-terminated polybutadiene (HTPB) (Krasol LBH-P, 2000) and liquid carboxyl-terminated polybutadiene (CTPB) (Ricon 131MA10) were provided from Sartomer Company Inc. Cobalt acetate (CoAc) used as inorganic filler for activating N-MXD6 was provided from Artenius UK. The molecular structures of the materials used are given in Table 2.1.

Materials	Molecular structure
PET	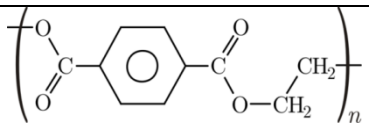
PET-co-10I	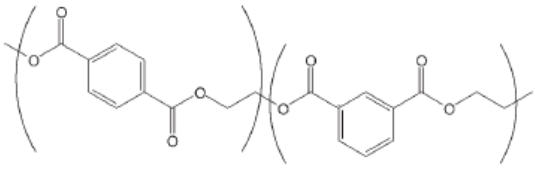
N-MXD6	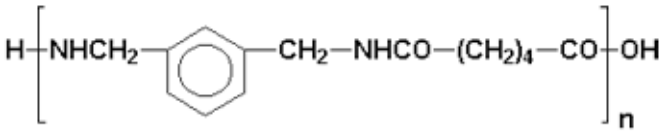
PET-co-5SIPA	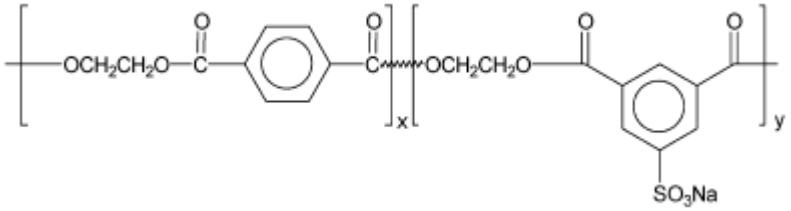
CTPB	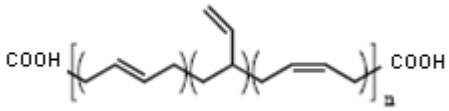
HTPB	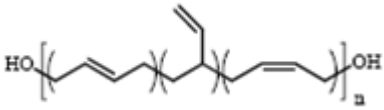
CoAc	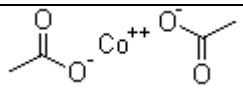

Table 2.1- Molecular structures of the materials used.

2.2. Blend and Film Preparation

PET was dried at 175°C for 6 hours in an air-circulating oven. N-MXD6 (85°C overnight) and PET-co-5SIPA (175°C for 14 hours) were dried in vacuum. Dried granules were placed in metal drums that were purged with nitrogen. PET/N-MXD6 blends have been prepared with Leistritz Micro 27-GL 44D twin screw extruder with 27 mm screw diameter and L/D ratio of 44. Screw speed was 100 rpm and throughput 4,5kg/h.

Scientific single screw extruder type LE25-30/CV with scientific laboratory cast film and sheet attachment type LCR-300 (Labtech Engineering) was used to produce cast films.

L/D ratio of the cast film machine is 25. PET films were prepared at 270 ºC. Chill roll was set to 65 °C for PET blends. The screw speed was adjusted to 60 rpm. The extruded blends were dried at 120 °C overnight before film casting and fed into the hopper of the cast film machine (Figure 2.1).

Figure 2.1- Laboratory Scale Cast Film Machine LE25-30/CV.

2.3. Thermal Analysis

A Netzsch DSC 204 was used to determine the thermal properties of the neat materials and the blends. First and second heating scans were performed by heating from 20°C to 300°C with a heating rate of 5°K/min. In between two heating scans samples were cooled to 20°C with a cooling rate of 40°K/min. In isothermal step samples were kept at 300°C (after first heating scan) and 20°C (after cooling) for 5 min to obtain a homogeneous temperature distribution.

Thermal stability and decomposition characteristics of the polymers were analyzed by using a Netzsch 449C thermo gravimetric analyzer (TGA). TGA analysis was done in the following manner; the samples were heated up to a temperature 600^{o}C with 10°K/min heating rate under nitrogen atmosphere and the mass loss of the samples was recorded against temperature.

2.4. Morphological Analysis

The blend samples were cryogenically fractured with liquid nitrogen. Etched samples were prepared by immersing them in formic acid for 72 hours, then rinsing with clean formic acid and immersing for an additional 24 hours. Finally the films were rinsed with water and dried. Thin films which do not break in liquid nitrogen were embedded in an acrylic resin, the surface thereof being trimmed with a microtome.

Morphologies of the fractured surfaces were investigated by a Leo G34-Supra 35VP scanning electron microscope (SEM) operating with an accelerating voltage of 1- 5 kV after they were coated with thin carbon film in an Emitech K950X sputter coater to avoid charge build up.

2.5. Gas Permeability Analysis

Barrier properties of the films were evaluated using Labthink TOY-C2 film-package oxygen permeability tester (designed in accordance with ASTM D3985, ASTM F1307, ASTM F1927) and Labthink TSY-T3 water vapor permeability tester (designed in accordance with ASTM E96, ASTM D1653). The oxygen permeability test, working on equal pressure method principle, was done at 25°C and 0 % RH conditions and the results were expressed as ml.cm/m^2.day. The water vapor permeability test, working on the principle of cup method, was performed at 38°C with a relative permeability of 90 % RH, and the results were expressed as grams of vapor permeated through the film as g.cm/m^2.day.

2.6. Molecular Weight Analysis

Intrinsic viscosity (IV) measurements were performed in Advansa Sasa Polyester San. A.Ş. 2 gram of sample was dissolved in 25 gram orto-chlorophenol for 15 minutes at 125ºC. The solution was then placed in Cannon Fenske Viscometer at 25 ºC and viscosity values were recorded.

2.7. Orientation Studies

Cast films were stretched simultaneously and biaxially by using an Iwamoto biaxial stretcher (Figure 2.4) with a stretch rate of 1 mm/sec in Polymer Engineering Division of University of Akron. The temperature during stretching was 90°C. Samples were prepared as a 13x13 cm square and placed in between hydraulic clamps shown in Figure 2.2. In order to distribute heat homogenously samples were kept at 90°C before stretching for 15 min. Engineering stress strain data was recorded during stretching. Draw ratio λ is defined as the ratio of the extended length to the original length. Samples were stretched 2 and 3 times their original dimensions (λ=2, λ=3).

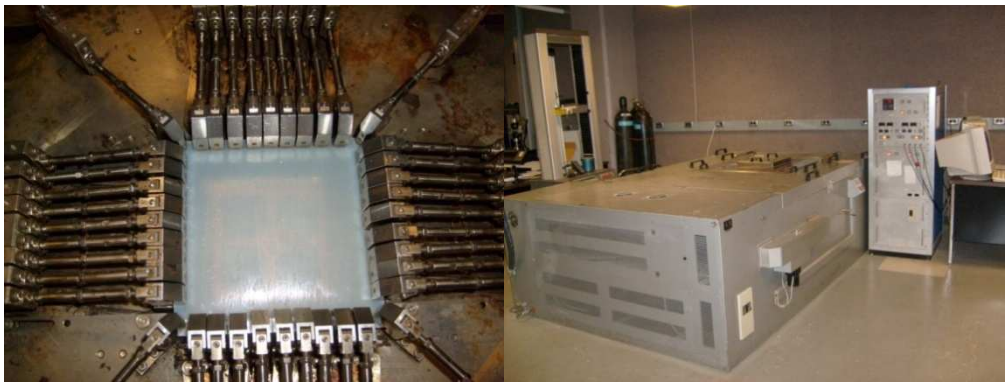

Figure 2.2- Iwamoto biaxial stretcher.

The uniaxial stretching experiments were carried out by using a custom made spectral-birefringence stretching machine (Figure 2.3) in University of Akron which records stress and strain values (both engineering and true) and birefringence during stretching. The measurements were performed at 90°C with a strain rate of 20 mm/sec.

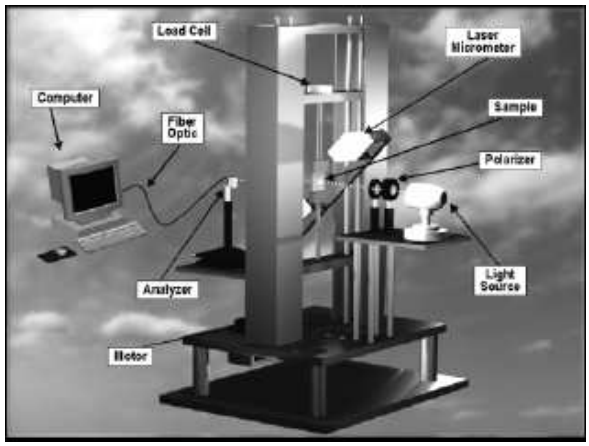

Figure 2.3- Spectral-birefringence stretching machine [67].

CHAPTER 3

3. RESULTS AND DISCUSSION

3.1. Blend and Film Preparation Parameters

In order to determine the working temperatures for extrusion, thermal properties of the raw materials were examined. Figure 3.2 shows the DSC thermograms of the materials used. Melting temperatures (Tm) of the matrix polymers are 249°C for PET and 229°C for PET-co-10I. As explained previously 10 wt.% isophthalic acid in PET-co-10I, hinders crystallization and decreases melting temperature. Tm of the dispersed phase (N-MXD6) is 238°C which is close to PET that makes it suitable for blending with PET. Tm of PET-co-SIPA is 247°C. HTPB and CTPB do not have melting temperatures since they are liquid. Extruder heating temperatures are generally arranged to be 15-20°C higher than the melting temperature of the polymers used. Therefore the blends were prepared with the heating profile shown in Figure 3.1 (the first and the last barrels at 275°C and the remaining at 265°C).

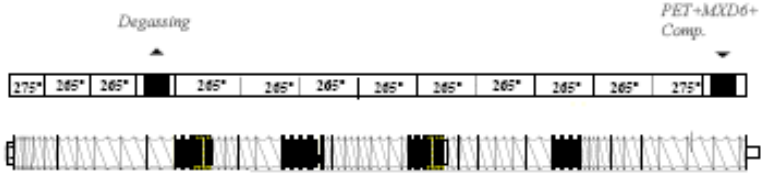

Figure 3.1- Temperature profile of the co-rotating intermeshing twin screw extruder.

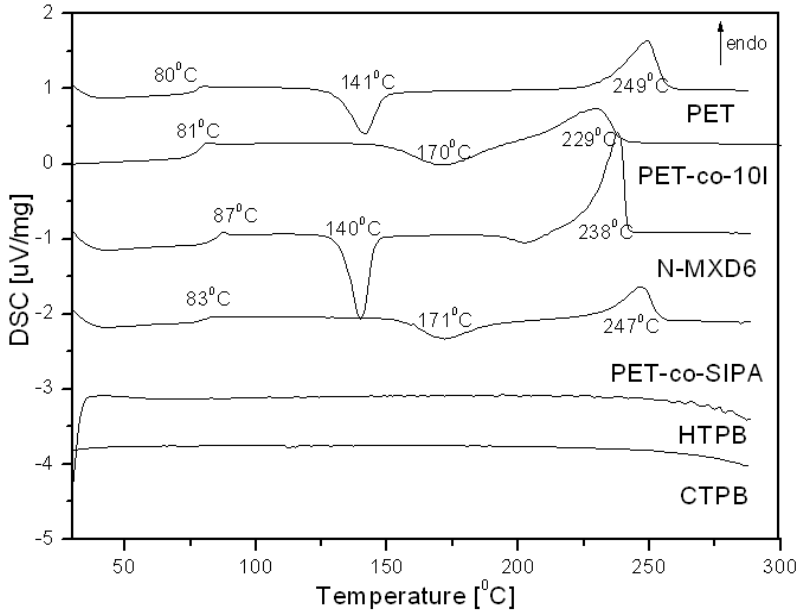

Figure 3.2- DSC thermograms of the materials used (2nd heating scan, 5ºK/min).

Glass transition temperatures of the raw materials are similar to each other, with Tg of PET being 80°C, PET-co-10I 81°C, N-MXD6 87°C, and PET-co-SIPA 83°C. Cold crystallization temperatures for PET and N-MXD6 are also similar being 141°C and 140°C respectively. PET-co-10I has a peak of cold crystallization temperature at 170°C and PET-co-SIPA at 171°C.

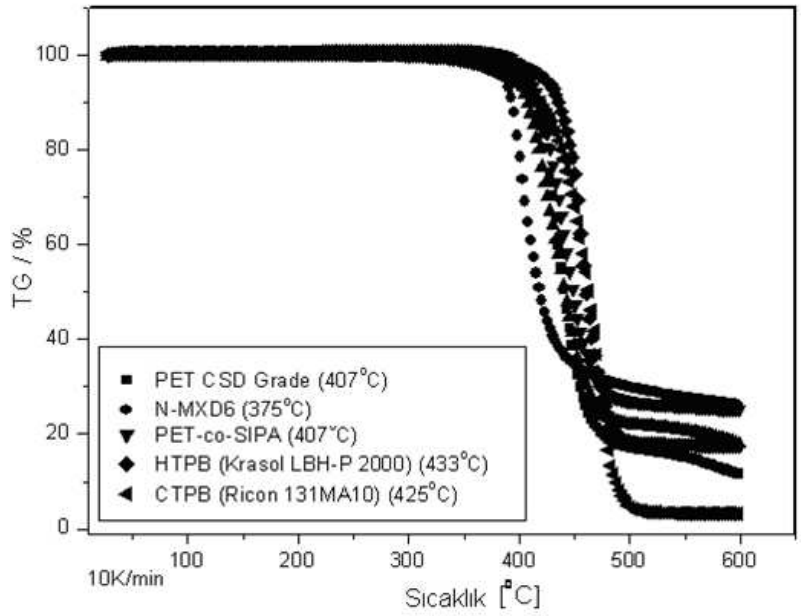

Figure 3.3- TGA of the materials used (Heating rate, 10 ºK/min).

In order to avoid working close to the decomposition temperatures (above which chemical degradation occurs) of the polymers used, thermo gravimetric analysis (TGA) was employed (Figure 3.3). The results show that the decomposition temperatures of the polymers (375-433°C) are much higher than the processing temperature (265°C).

Intrinsic viscosity (IV) is an important parameter for plastic processing in industry. Specific IV values must be provided in order to produce high quality products. PET and PET-co-10I that were used in this project have an IV of 0,82 dl/g. Starting from this value, after each step ("granule" after extrusion and "film" after film casting), changes in IV values of the blends were determined. As explained in the introduction section, the necessary IV for film production is on average 0,65 dl/g. The blends after extrusion have 0,7-0,74 dl/g of IV as shown in Table 3.1 which was sufficient to produce high quality films. During extrusion process feed hopper was purged with high purity nitrogen gas (99,999% N_2 gas, max 2 ppm oxygen and max 3 ppm moisture) and wrapped with a polyethylene film in order to prevent oxygen coming into contact with PET chips and thus preventing hydrolytic degradation of PET. Nonetheless, IV values after production of cast films were very low ranging from 0,42 to 0,67 dl/g as no precautions to avoid oxygen contact from PET have been taken like purging with nitrogen or covering hopper with PE film. On industrial scale PET is transformed to extruder feed hopper through dehumidifier driers without air contact to avoid hydrolytic degradation.

sample	granule	film	sample	granule	film
PET	0,735	0,676	PET-co-10I	0,730	0,653
EP100	0,728	0,512	EO100	0,742	0,487
EP101	0,735	0,426	EO101	0,700	0,455
EP102	0,724	0,552	EO102	0,704	0,544
EP103	0,710	0,504	EO103	0,721	0,442
EP104	0,708	0,506	EO104	0,714	0,526
EP105	0,718	0,511	EO105	0,706	0,512

Table 3.1- IV values of the blends in dl/g.

3.2. Thermal Behavior of Blends

In order to understand the effects of extrusion on the blends, first heating scans have been considered as shown in Figure 3.4. Glass transition temperatures (Tg) of the extruded PET and N-MXD6 are respectively 74°C and 85°C. Tg of PET/N-MXD6 (EP100) blend gives a single peak at 73°C, which proves that N-MXD6 does not affect the Tg of the blend since its percentage (5 wt. %) is relatively small in the blend. Extruded PET has a melting temperature of 253°C and a cold crystallization temperature of 125°C. Extruded N-MXD6 has a melting temperature of 238°C and a cold crystallization temperature of 125°C. In general, addition of a second phase to the PET matrix decreases its cold crystallization temperature. However, no significant change has been observed for cold crystallization temperatures of PET/N-MXD6 blends with or without compatibilizers (Figure 3.4). A small shoulder peak near the melting peak of PET blends corresponds to the melting temperature of N-MXD6. This indicates the incompatibility between PET and N-MXD6. In the presence of PET-co-SIPA as compatibilizer in blends (EP101, EP103 and EP105), this shoulder peak disappears, which reveals the efficiency of PET-co-SIPA as a compatibilizer in PET/N-MXD6 blends.

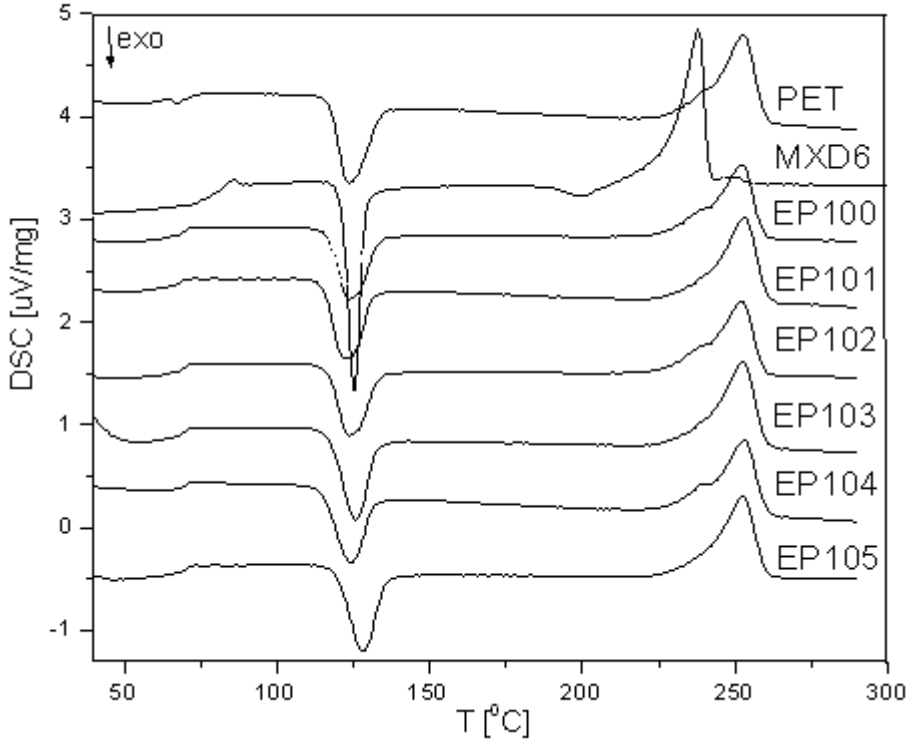

Figure 3.4- DSC thermograms of extruded blends with matrix polymer PET. (1^{st} heating scans, heating rate: 5ºK/min)

PET-co-10I has a glass transition temperature of 78°C, cold crystallization temperature of 135°C and melting temperature of 240°C (Figure 3.5). PET-co-10I/ N-MXD6 blends show a single Tg at 78°C. Unlike PET/N-MXD6 blends, no shoulder peak for N-MXD6 in the blends of PET-co-10I/N-MXD6 is observed which indicates the compatibility of PET-co-10I and N-MXD6 with or without the presence of compatibilizer. Nucleation effect of N-MXD6 is observed to decrease the cold crystallization temperature for the blends containing compatibilizers. Cold crystallization peak of PET-co-10I (135°C), reduced to 128°C for EO101, EO103, and EO104, to 126°C for EO102, to 133°C for EO105.

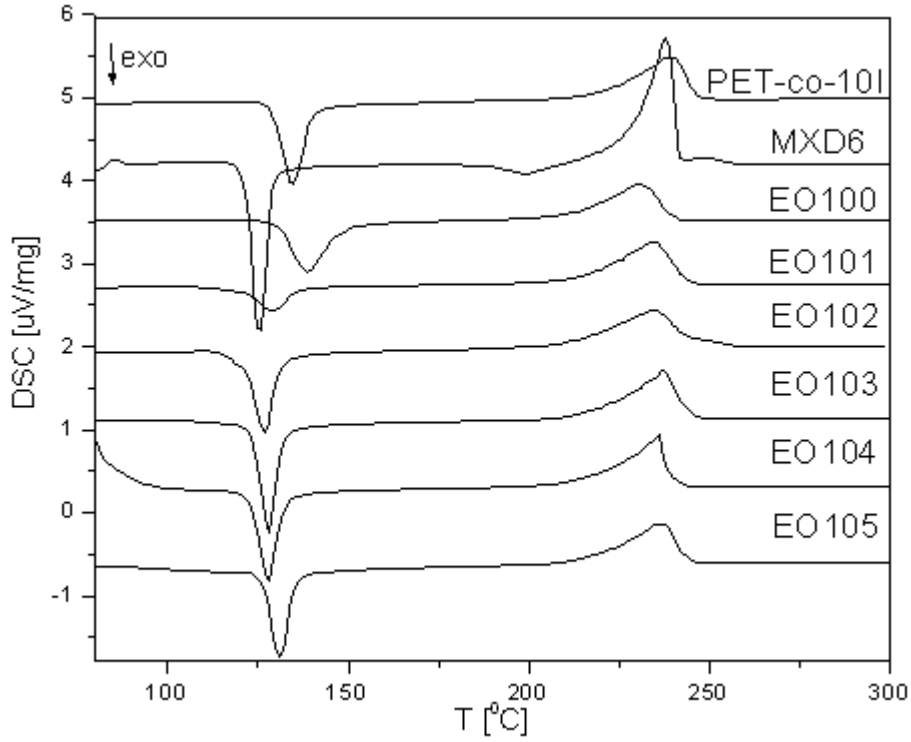

Figure 3.5- DSC thermograms of the extruded blends with matrix polymer PET-co-10I. (1^{st} heating scans, heating rate: 5ºK/min).

3.3. Morphology of the Blends

SEM images of the blends prepared by twin screw extrusion are shown in Figure 3.6. Spherical N-MXD6 particles were observed to be dispersed in PET matrix. Particle sizes of N-MXD6 in the blends containing different compatibilizers are summarized in Table 3.2. Accordingly PET/N-MXD6 (95/5 w/w) blends without compatibilizer gave out a coarse morphology with particles of 2 μm average size, which refers to their incompatibility. After addition of different compatibilizers and combinations as shown in the Table 3.2, particle size of the dispersed phase reduced. The smallest particle size of 0,1 μm has been observed for the blends which contain PET-co-5SIPA as compatibilizer. Efficiency of PET-co-SIPA as compatibilizer is a result of strong interactions like ion-dipole interactions or transesterification reactions between sulfonated ionomers and polyamides [24]. CTPB alone or with HTPB (EP102 and EP104) decreased particles size to 0,4-0,5 μm. The aim of using CTPB and HTPB is the ability of oxygen binding due to carbon double bonds in their structure. Incorporation of CTPB and HTPB with PET-co-SIPA reduced the particle size further to 0,16 μm (EP103 and EP105) since HTPB and CTPB provide active oxygen barrier properties to these blends due to their ability of oxidation with carbon- carbon double bonds.

Notation	Blends	% wt	Particle Size / μm
EP100	PET/N-MXD6	95/5	2
EP101	PET/N-MXD6/PET-co-5SIPA/CoAc	85.5/5/9.5/250ppm	0,10
EP102	PET/ N-MXD6/CTPB/CoAc	94/5/1/250ppm	0,40
EP103	PET/ N-MXD6/CTPB/PET-co-5SIPA/CoAc	84.5/5/1/9.5/250ppm	0,16
EP104	PET/ N-MXD6/CTPB+HTPB(1/2)/CoAc	94/5/1/250ppm	0,45
EP105	PET/N-MXD6/CTPB+HTPB(1/2)/ PET-co-5SIPA/CoAc	84.5/5/1/9.5/250ppm	0,16

Table 3.2- Particle size of the dispersed phase N-MXD6 in PET matrix.

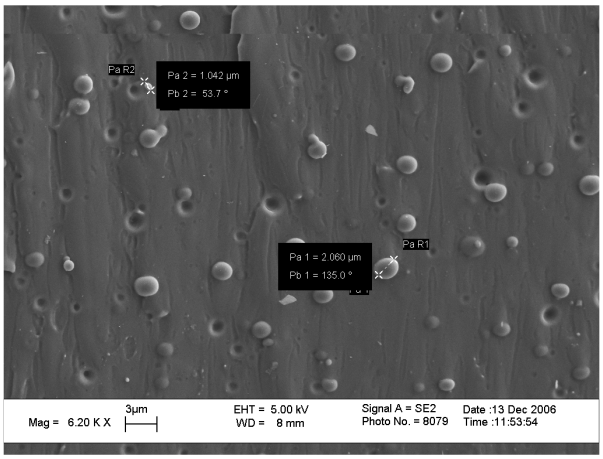

EP100
Particle Size: 2µm

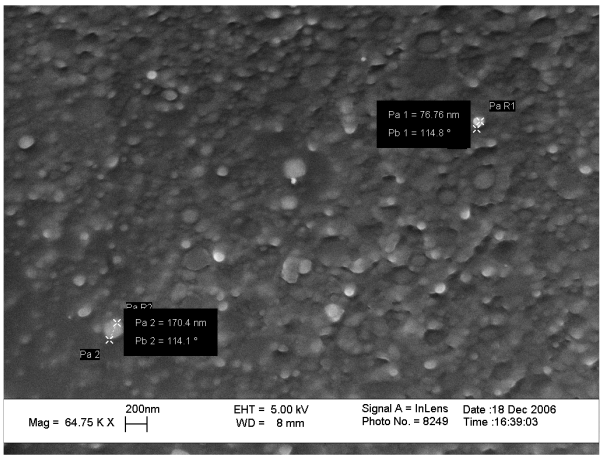

EP101
Particle Size: 0,1 µm

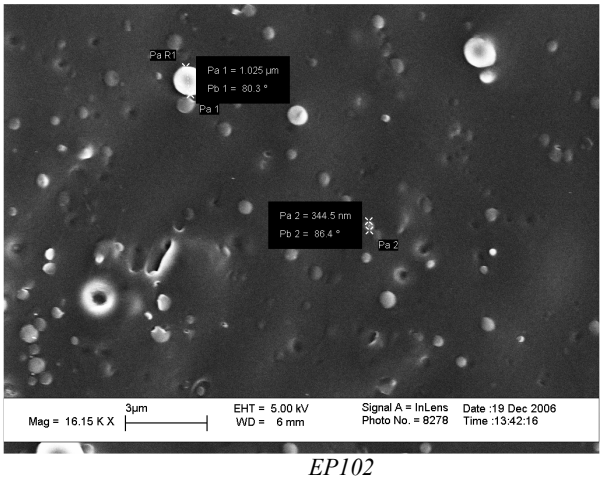

EP102
Particle Size: 0,4 µm

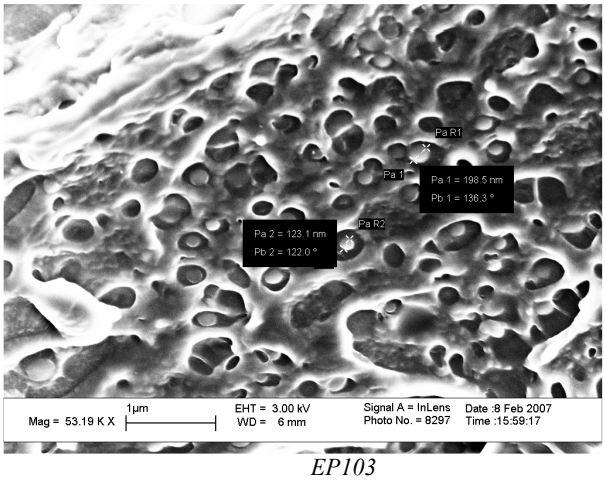

EP103
Particle Size: 0,12-0,2 (0,16) µm

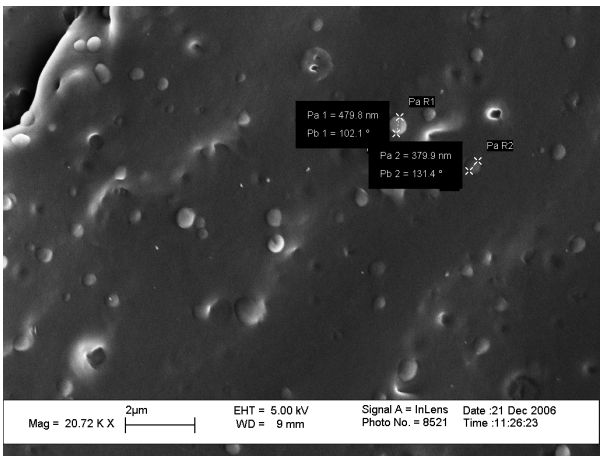

EP104
Particle Size: 0,4-0,5 (0,45) µm

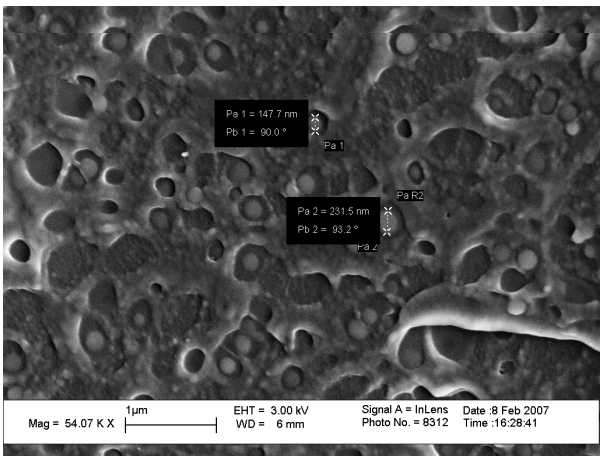

EP105
Particle Size: 0,15-0,23 (0,19) µm

Figure 3.6- SEM images of the PET/N-MXD6 blends with different compatibilizers.

Replacing PET with PET-co-10I which consists of 10 wt. % IPA resulted in a particle size of 0,3 μm for N-MXD6 without any compatibilizer as shown in Table 3.3. Dispersion of N-MXD6 in PET-co-10I matrix is given with SEM images in Figure 3.7. Carboxyl (-COOH) group of isophthalic acid in PET-co-10I and methylene ($-CH_2$) group of N-MXD6 bind to the benzene ring in meta position. Therefore meta-phenylene linkage that both N-MXD6 and PET-co-10I have resulted in better compatibility in comparison to the PET/N-MXD6 blend. The addition of compatibilizers reduced the N-MXD6 particle size to 0,15 μm for EO101 blend. CTPB addition as a compatibilizer did not change the particle size (EO102). Using both CTPB and HTPB at the same time results in a small reduction in particle size to 0,21 μm (EO104). Incorporation of CTPB, HTPB and PET-co-SIPA together (EO103, EO105) as compatibilizers did not provide any further reduction in particle size in comparison to the usage of PET-co-5SIPA alone.

Notation	**Blends**	**% wt**	**Particle Size / μm**
EO100	PET-co-10I/N-MXD6	95/5	0,30
EO101	PET-co-10I/N-MXD6/PET-co-5SIPA/ CoAc	85.5/5/9.5/250ppm	0,15
EO102	PET-co-10I/ N-MXD6/CTPB/CoAc	94/5/1/250ppm	0,30
EO103	PET-co-10I/ N-MXD6/CTPB/PET-co-5SIPA/ CoAc	84.5/5/1/9.5/250ppm	0,17
EO104	PET-co-10I/ N-MXD6/CTPB+HTPB(1/2)/CoAc	94/5/1/250ppm	0,21
EO105	PET-co-10I/N-MXD6/CTPB+HTPB(1/2)/ PET-co-5SIPA/ CoAc	84.5/5/1/9.5/250ppm	0,15

Table 3.3- Particle size of the dispersed phase N-MXD6 in PET-co-10I matrix.

The smallest particle size was obtained for EP101 (0,1 μm) and EO101 (0,15 μm) blends that both contain PET-co-5SIPA as the compatibilizer. The efficiency of PET-co-5SIPA as compatibilizer is attributed to the fact that sulfonated ionomers interact strongly with aliphatic polyamides, establishing a network structure in which sulfonated anions coordinate to amide N-H groups, whereas the counter ions complex to multiple amide carboxyl oxygen groups [34]. The use of sulfonated ionomers as compatibilizers for PET and aliphatic polyamides are widely studied. The results obtained in this study prove that sulfonated ionomers are also efficient compatibilizers with aromatic polyamides.

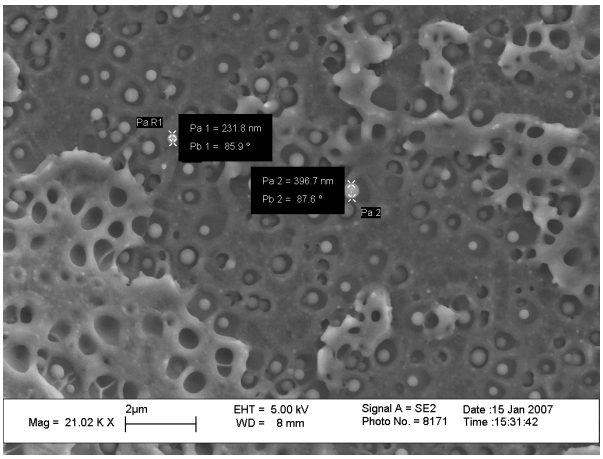

EO100
Particle Size: 0,2-0,4 (0,3) µm

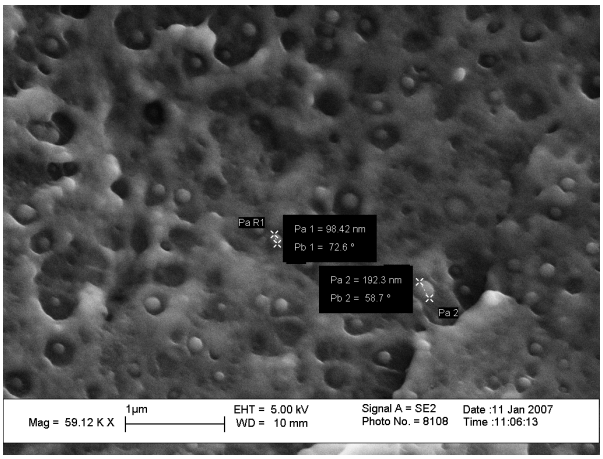

EO101
Particle Size: 0,1-0,2 (0,15) µm

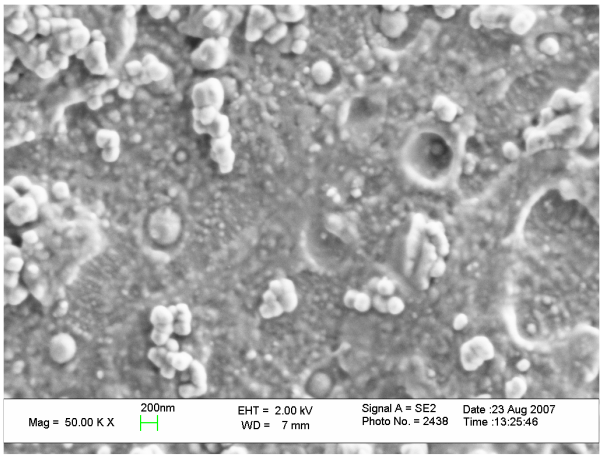

EO102
Particle Size: 0,22-0,38 (0,3) µm

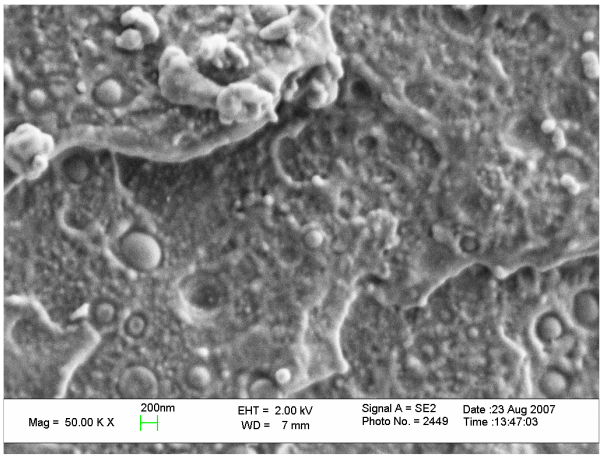

EO103
Particle Size: 0,1-0,24 (0,17) µm

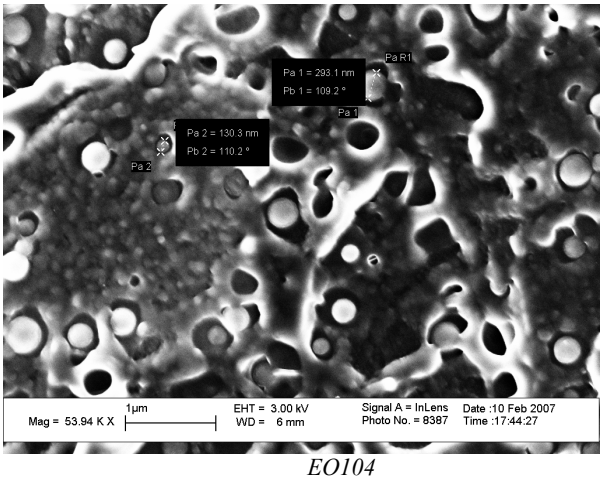

EO104
Particle Size: 0,13-0,29 (0,21) µm

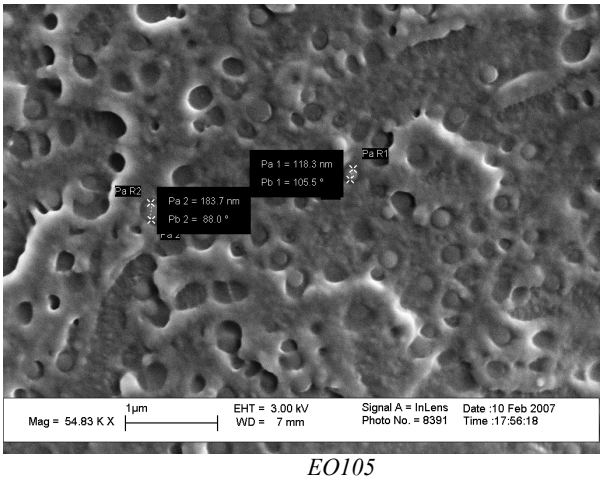

EO105
Particle Size: 0,12-0,18 (0,15) µm

Figure 3.7- SEM images of PET-co-10I/N-MXD6 blends with different compatibilizers.

3.4. Gas Permeability

Oxygen permeability measurements of the films were performed by using Labthink TOY-C2 Film-Package Oxygen Permeability Tester. The results of the unoriented cast film and the biaxially stretched (2x and 3x) films are given in Table 3.4. According to permeability results it is obvious that oxygen permeability values of pure PET and PET-co-10I films are quite similar to each other being respectively 0,38 and 0,36 ml.cm/m^2.day. Addition of high barrier N-MXD6 and compatibilizers decreased oxygen permeability as expected. The highest amount of decrease is observed at EP104 for PET blends (31% reduction compared to pure PET), at EO103 for PET-co-10I blends (63% reduction compared to pure PET-co-10I). Generally effect of biaxial stretching leads to reduction of oxygen gas permeability except some PET-co-10I blends where oxygen gas permeability increased after stretching (EO102, EO103, EO104). Oxygen gas permeability of the PET blends decreased significantly after stretching. Reduction of 63% in oxygen permeability was observed for EP102 which was stretched two times its original dimensions (biaxial 2x). 3x stretching resulted in an increase of permeability for most of the blends as shown in Figure 3.8, which shows that stretching above 2x is breaking the chain orientation and creating micro voids or permeable areas inside the structure. In exclusive manner oxygen permeability of EP101 blends has been decreased with 3x stretching by 59% compared to non-stretched blend due to its high compatibility so the stretching does not result in cracks or voids.

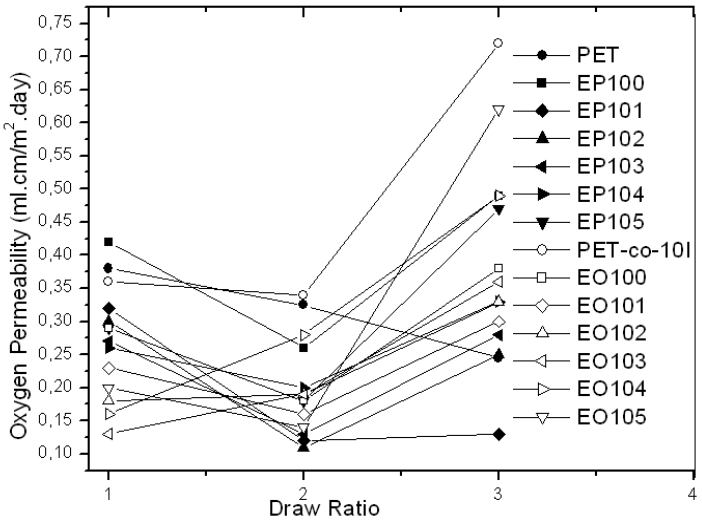

Figure 3.8- Relationship between oxygen permeability and draw ratio for the blends.

Water vapor permeability tests of the films were performed by using Labthink TSY-T3 water vapor permeability tester that works with a gravimetric method. In general unoriented PET-co-10I blends have lower permeability values compared to PET blends. Pure PET film has a water vapor permeability of 0,252 g.cm/m^2.day, while pure PET-co-10I has a value of 0,102 g.cm/m^2.day. Addition of N-MXD6 and compatibilizers also has a different effect on PET and PET-co-10I blends. Water vapor permeability of PET films decreased with the addition of Nylon and compatibilizer. The most striking reduction of 51% compared to pure PET was observed when CTPB and PET-co-5SIPA were used together as compatibilizers (EP103). Water vapor permeability of PET-co-10I blends decreased with the addition of nylon and compatibilizers. Biaxial stretching resulted in higher barrier properties against water vapor for pure PET blends with a 57% reduction at biaxial 2x, and 69% reductions at biaxial 3x stretched films compared to non-oriented PET. For the rest of the polymers no general trend has been observed with the biaxial stretching therefore it is not possible to make a comment on them (Figure 3.9).

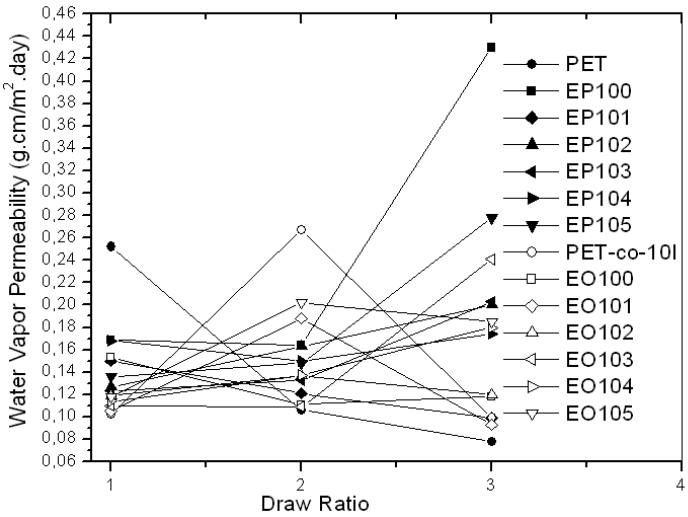

Figure 3.9- Relationship between water vapor permeability and draw ratio for the blends.

	Particle size (μm)	Oxygen Permeability (ml.cm/m^2.day)			Water Vapor Permeability (g.cm/m^2.day)			% Crystallinity			
Notation	Extruded granules	Cast Film	Film-Biaxial2X	Film-Biaxial3X	Cast Film	Film-Biaxial2X	Film-Biaxial3X	Cast Film	Film-Biaxial2X	Film-Biaxial3X	Film-Uniaxial
PET	-	0,388	0,325	0,245	0,252	0,106	0,078	11,08	17,42	28,66	36,48
EP100	2,00	0,420	0,261	0,493	0,169	0,164	0,430	16,10	14,56	21,88	27,69
EP101	0,10	0,324	0,120	0,127	0,150	0,121	0,099	20,49	16,16	14,88	27,09
EP102	0,40	0,298	0,114	0,253	0,127	0,163	0,200	10,61	12,41	11,35	8,81
EP103	0,16	0,270	0,127	0,281	0,123	0,133	0,203	13,24	14,24	12,27	25,42
EP104	0,45	0,256	0,203	0,326	0,168	0,150	0,174	12,06	11,59	17,11	11,03
EP105	0,16	0,293	0,176	0,473	0,136	0,148	0,278	13,14	9,59	13,70	14,47
PET-co-10I	-	0,356	0,339	0,722	0,102	0,267	0,099	4,22	19,76	13,32	26,74
EO100	0,30	0,293	0,179	0,375	0,153	0,111	0,118	16,81	10,19	11,70	6,96
EO101	0,15	0,233	0,158	0,300	0,105	0,188	0,093	10,62	10,62	10,92	11,13
EO102	0,30	0,178	0,190	0,330	0,119	0,137	0,120	3,89	9,00	10,58	20,58
EO103	0,17	0,130	0,191	0,356	0,110	0,109	0,241	5,75	6,29	0,17	5,67
EO104	0,21	0,163	0,283	0,488	0,114	0,137	0,180	4,88	4,48	8,21	9,32
EO105	0,15	0,198	0,140	0,622	0,118	0,202	0,185	6,84	6,82	4,47	7,65

Table 3.4- Particle size, permeability and crystallinity results of the blends.

3.4.1. Morphology and Barrier Properties

After biaxial stretching, morphologies of the N-MXD6 phase dispersed in PET matrix changed and gave out the laminar structures shown in Figure 3.10 for EP104 film. N-MXD6 spheres had an average radius of 0,1 μm. After stretching, the spheres transformed into ellipsoids with a thickness of 78-150 nm and length of 150-958 nm. Aspect ratio, the ratio of length to thickness for these nano-ellipsoids were in average 6. This structure created a tortuous pathway for the oxygen ingress and thus decreased the oxygen permeability of the blend. Both oxygen and water vapor permeability of EP104 film decreased after 2x biaxial stretching. Unoriented cast film has an oxygen permeability of 0,256 ml.cm/m^2.day, 2x film has 0,203 ml.cm/m^2.day. %31 reduction in oxygen permeability compared to pure PET (0,388 ml.cm/m^2.day) resulted from the tortuous pathway due to the laminar structure after 2x biaxially stretching. The same situation has been observed for water vapor permeability where cast film permeability decreased from 0,168 g.cm/m^2.day to 0,150 g.cm/m^2.day after 2x biaxially stretching. Both oxygen and water vapor permeability results increased with 3x stretching, which is thought to be a result of microvoids formed during stretching.

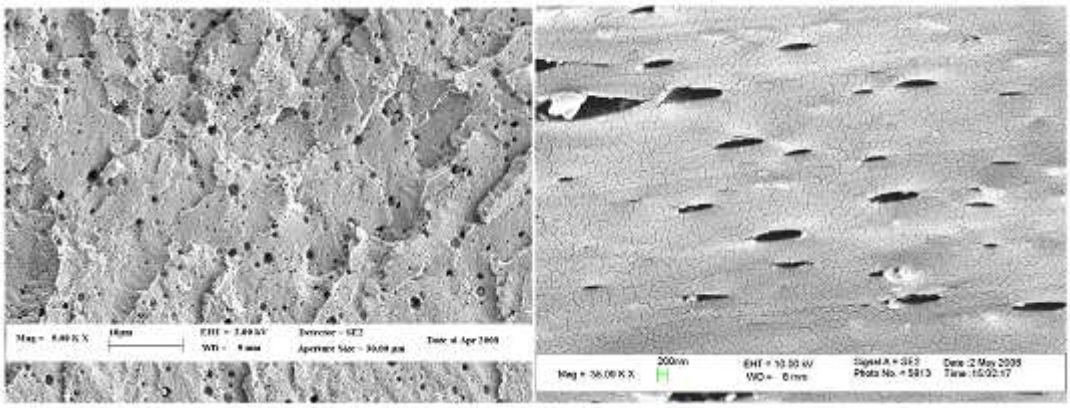

Figure 3.10- Morphology of the cross section of the films before and after stretching; a) unoriented cast film, b) 2x biaxial stretched film.

3.4.2. Biaxial Stretching and Barrier Properties

Biaxial stretching results in both chain alignment (orientation) and crystallization. As shown in Figure 3.11 and 3.12 oxygen permeability decreases with 2x stretching except for the films EO103-5. 3x stretching increased permeability for all the blends except PET. It is highly required to find out the optimum draw ratio for each blend. In this study only 2x and 3x were examined as draw ratios. According to results only PET behaved as expected (stretching decreased permeability continuously). For the other blends incompatibility of some areas and nonlinearity coming from meta linkage of N-MXD6 phase are thought to be the reasons for resistance to orientation and so an increase in permeability. On the other hand relationship between biaxial stretching and water vapor permeability is highly complex. Only PET, EP102 and EO100 showed a continuous reduction of permeability with biaxial stretching as shown in Figure 3.13-14.

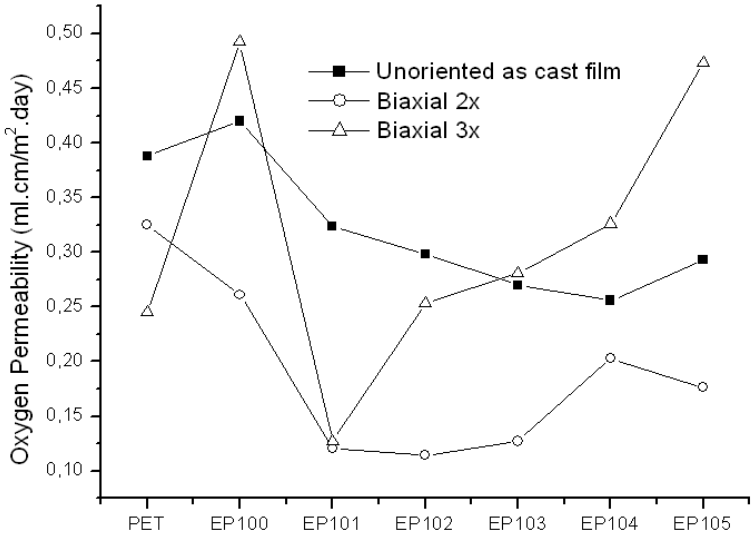

Figure 3.11- Effect of biaxial stretching on oxygen permeability of PET/N-MXD6 films.

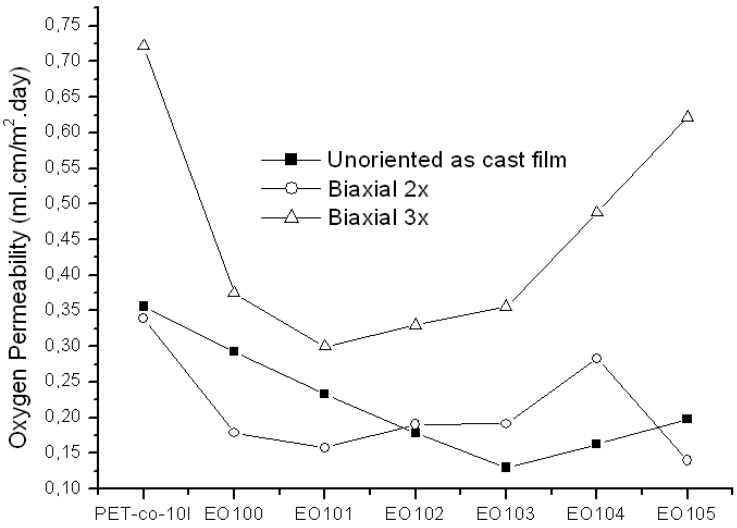

Figure 3.12- Effect of biaxial stretching on oxygen permeability of PET-co-10I/N-MXD6 films.

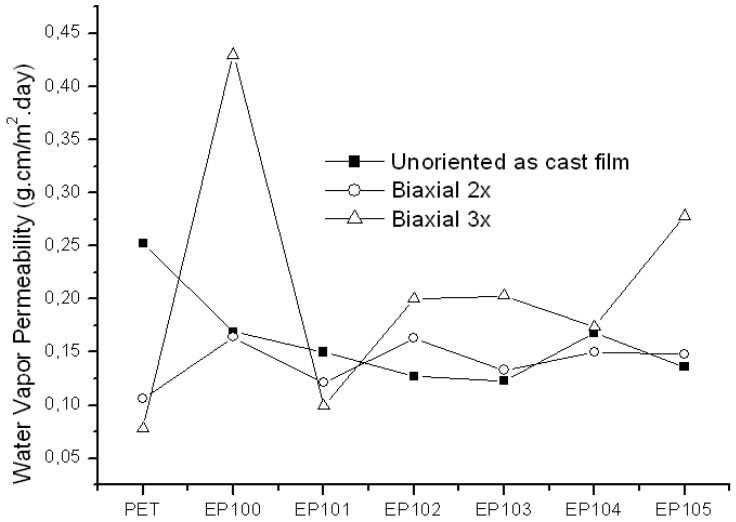

Figure 3.13- Effect of biaxial stretching on water vapor permeability of PET/N-MXD6 films.

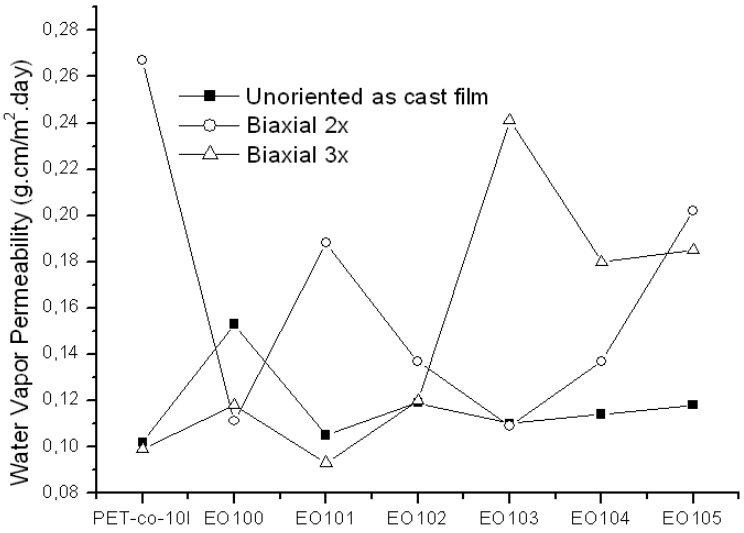

Figure 3.14- Effect of biaxial stretching on water vapor permeability of PET-co-10I/N-MXD6 films.

3.4.3. Crystallinity and Barrier Properties

Chain orientation during stretching of the films induces crystallization. The crystallization values of the films are shown in Table 3.4. There is no general trend in crystallinity for PET/N-MXD6 (Figure 3.15) and PET-co-10I/N-MXD6 (Figure 3.16) blends. Only PET, PET-co-10I and EO103 films have shown a continuous increase of crystallinity with stretching. Blending with N-MXD6 decreased the ability to crystallize of the films due to meta linkage of N-MXD6 hindering crystallization. This resulted a complex behavior of crystallization for the blends. Also the measurement of crystallinity has been performed with the samples taken from different sides of the films. Nonuniformity of the films could result in differences in crystallinity values obtained. Another important observation is that PET films crystallize more than PET-co-10I films. As seen in Figure 3.15 crystallization values of the PET films are in the range of 10 to 36 % while PET-co-10I blends crystallize in the range of 0,1 to 26 %. Meta linkage and the kink structure in PET-co-10I prevented chains from crystallization that resulted in lower crystallization degrees compared to PET.

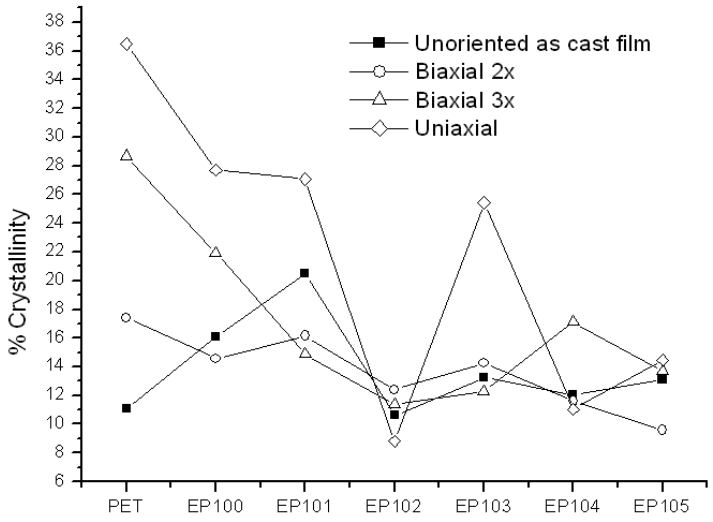

Figure 3.15- Effect of biaxial stretching on % crystallinity of PET/N-MXD6 films.

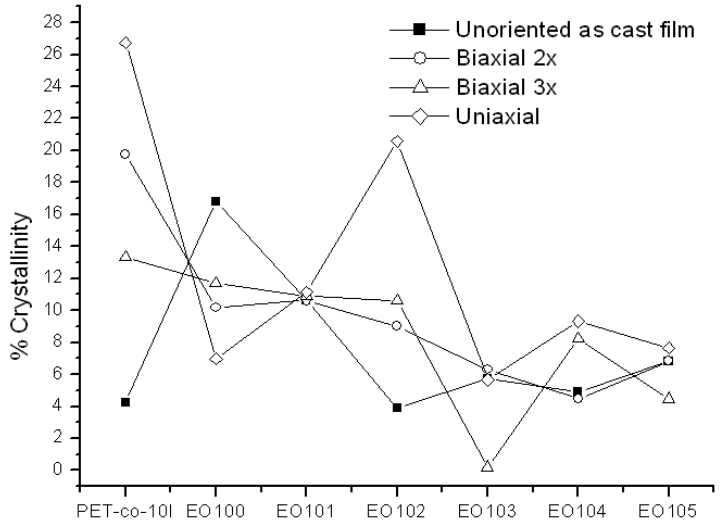

Figure 3.16- Effect of biaxial stretching on % crystallinity of PET-co-10I/N-MXD6 films.

Stretching increased crystallinity of pure PET films from 11,08% to 17,42% for biaxial 2x, to 28,66% for biaxial 3x stretched films as given with the DSC thermogram in Figure 3.17. Uniaxial stretching results in 36,48 % crystallinity for pure PET films as strain rate of uniaxial stretching was 20 mm/sec while biaxial stretching was 1 mm/sec. The effects of drawing on the thermal cold crystallization are the decrease of Tcc and the reduction in the area of the Tcc peak resulting from the pre-orientation of the molecular chains. Strain induced crystallization reduces the ability to crystallize during DSC heating [28]. These effects have been observed in Figure 3.17 with the reduction

in area of Tcc and a decrease of Tcc with the draw ratio. As explained in detail in the introduction, crystalline parts are impermeable to gases, therefore permeability decreased with increase in crystallinity for PET films as shown in Figure 3.18.

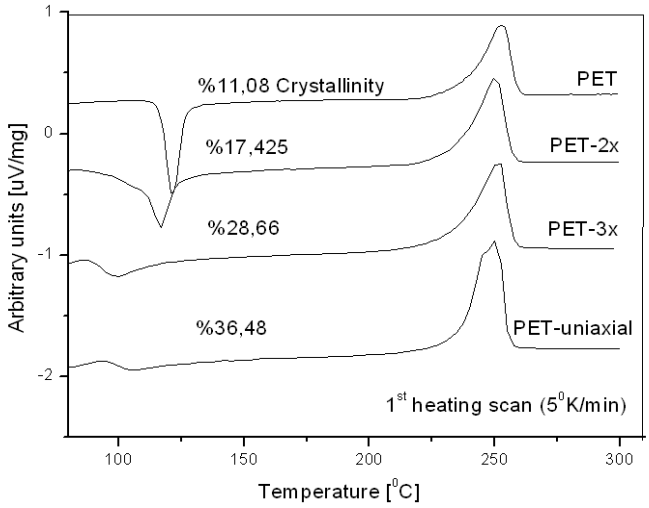

Figure 3.17- DSC thermograms of as cast PET, 2x and 3x biaxial and uni-axial oriented PET.

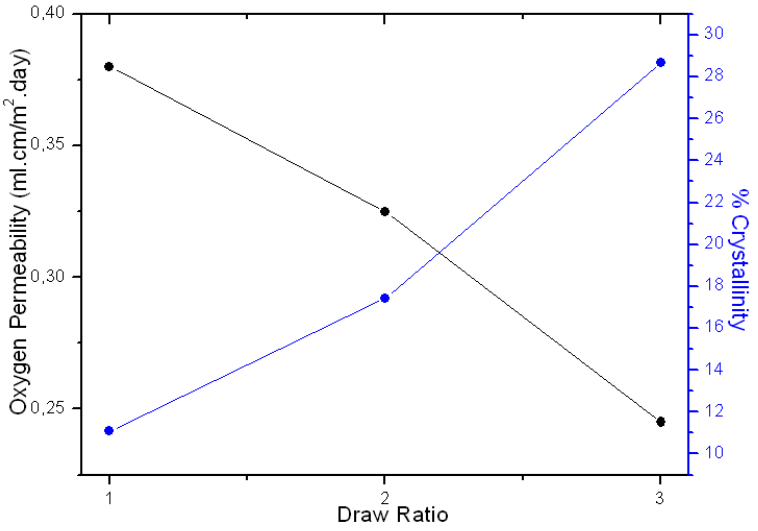

Figure 3.18- Relationship between draw ratio, % crystallinity and oxygen permeability of PET film.

3.4.4. Chemistry and Barrier Properties

Incorporation of 10 wt. % isophthalic acid during polymerization of PET tends to decrease oxygen permeability of the blends as listed in Table 3.4. There has been observed no significant difference in terms of oxygen gas permeability when compared unoriented cast film of pure PET and PET-co-10I which are 0,38 and 0,36 ml.cm/m^2.day respectively. On the other side, films of unoriented as cast PET-co-10I/N-MXD6 have lower permeability values than PET/N-MXD6 blends. Permeability values drop from 0,42 (EP100) to 0,29 (EO100) ml.cm/m^2.day with the addition of isophthalic acid. Compatibilized blends also gave the same results; reduction in permeability from 0,32 (EP101) to 0,23 (EO101), from 0,30 (EP102) to 0,18 (EO102, from 0,27 (EP103) to 0,13 (EO103), from 0,26 (EP104) to 0,16 (EO104), from 0,29 (EP105) to 0,20 (EO105) ml.cm/m^2.day.

Results of water vapor permeability of the films indicated the same trend. PET has water vapor permeability of 0,252 g.cm/m^2.day while addition of isophthalic acid reduced this to 0,102 g.cm/m^2.day for PET-co-10I. Permeability values decreased from 0,169 (EP100) to 0,153 (EO100) with the addition of isophthalic acid. Compatibilized blends also gave the same results; reduction in permeability from 0,150 (EP101) to 0,105 (EO101), from 0,127 (EP102) to 0,119 (EO102), from 0,123 (EP103) to 0,110 (EO103), from 0,168 (EP104) to 0,114 (EO104), from 0,136 (EP105) to 0,118 (EO105) g.cm/m^2.day. Insertion of isophthalic acid changes para linkage to a meta linkage of the phenyl ring of PET. N-MXD6 also has meta linkage. Therefore N-MXD6 and PET-co-10I are already compatible to some extend even without employing a compatibilizer. This compatibilization and the decreased linearity of PET by meta linkage that does not allow gas permeation with the suppression of flipping of the phenyl rings resulted in low permeability for oxygen and water vapor permeability of some of PET-co-10I blends studied in this thesis even though their crystallinity degrees are not as high as PET blends. For instance EO100 blends have lower permeability than EP100 blends even though the crystallinity of EP100 blends after stretching are higher than EO100 as shown in Figure 3.19. On the other hand for other PET-co-10I blends stretching resulted in higher permeability values compared to PET blends. Lower permeability values that PET blends obtained are the result of better crystallinity of PET blends than PET-co-10I blends which surpasses the effect of chemical compatibility.

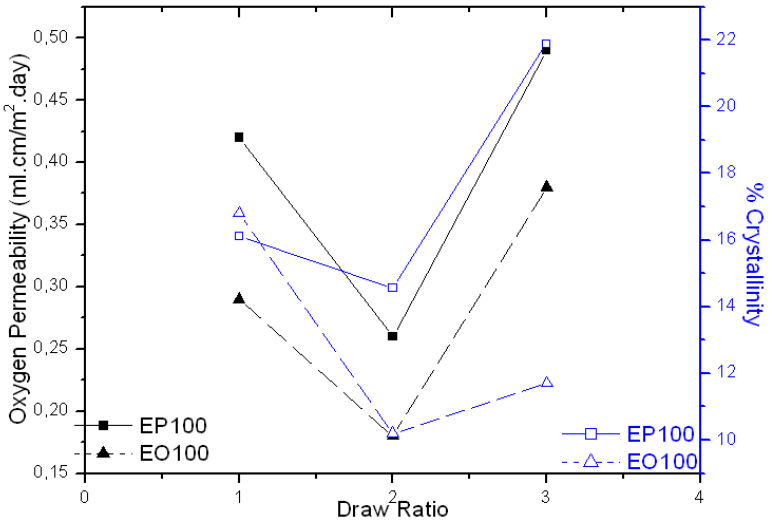

Figure 3.19- Comparison of oxygen permeability and % crystallinity of EP100 and EO100 blends.

3.5. Mechano-optical Properties of the Blends

Refractive index (RI) of PET and PET-co-10I is 1,5735 and RI of N-MXD6 is 1,5773 [20]. Birefringence or optical anisotropy is defined as the refractive index difference between stretch and thickness directions. Uniaxial stretching increases the refractive index in the stretch direction and decreases the refractive index in the thickness direction. Therefore during stretching birefringence increases. Uniaxial stretching has just been performed at 90ºC with strain rate of 20 mm/sec. In all the films studied with uniaxial stretcher only PET, PET-co-10I and EP103 films showed a typical crystallization behavior of PET. Alignment of PET chains during stretching gives rise to high birefringence and also causes strain induced crystallization. In Figure 3.20 the first slope corresponds to the nucleation of crystallites, the second slope shows the region of growth of the crystallites. The final third slope is the region for stabilization of the crystallites.

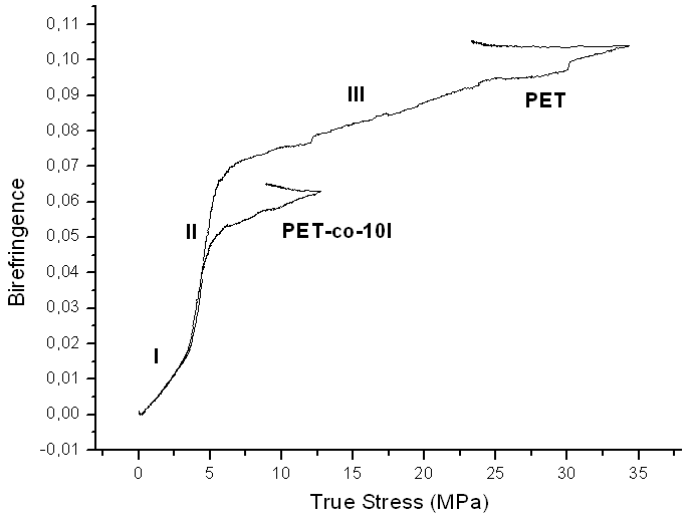

Figure 3.20- Birefringence vs. True Stress for PET and PET-co-10I.

Large birefringence of PET in Figure 3.20 is attributed to the high degree of molecular orientation that can be achieved with the linear configuration of the backbone aromatic rings [20]. At first in Figure 3.20 there was no difference between PET and PET-co-10I, however further stretching caused lower birefringence in PET-co-10I due to suppression of molecular orientation by meta substitution of aromatic ring of isophthalic acid in PET-co-10I. Figure 3.21 shows the same effect of meta linkage on molecular orientation by resulting in a small birefringence in a PET/N-MXD6 blend. Meta linkage in N-MXD6 hinders crystallization in EP103 blends that causes small difference in refractive indexes in stretch and transverse directions. With an appropriate strain rate PET-co-10I (EO series) blends are thought to result in small birefringence change due to meta linkages of both N-MXD6 and PET-co-10I.

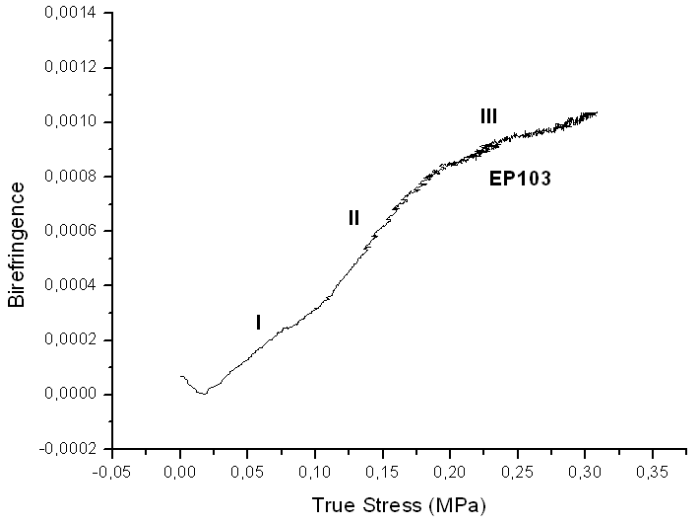

Figure 3.21- Birefringence vs. True Stress for EP103 blends.

The upswing in the stress strain curves of polyesters (Figure 3.22) refers to the strain hardening which is quite important in blow molding and orientation studies. The rise in strain causes less time for the relaxation of polymer chains that provides higher orientation and alignment of the polymer chains. This results in structural order among the macromolecules and leads to strain induced crystallization [68]. As seen in Figure 3.22 strain-induced crystallization occurs between strain values of 3 and 3,75 for PET and 4,5 and 5,25 for PET-co-10I. Retardation of crystallization for PET-co-10I is related again to the meta linkages in isophthalic acid which hinders crystallization. This situation causes a drawback for industrial applications of PET-co-10I as higher strain values are required to obtain sufficient stress for orientation of the molecules. Stress strain curves of the blends of PET/N-MXD6 and PET-co-10I/N-MXD6 blends are given in Figure 3.23 and 3.24 respectively. N-MXD6 hinders crystallization due to its meta linkages like PET-co-10I therefore blends did not show strain hardening. Exceptionally EP104 was the only blend which shows strain induced crystallization. The reason of this is thought to be the interactions in between CTPB+HTPB and N-MXD6. PET-co-10I blends showed no strain hardening due to the combined effect of meta linkages in both PET-co-10I and N-MXD6.

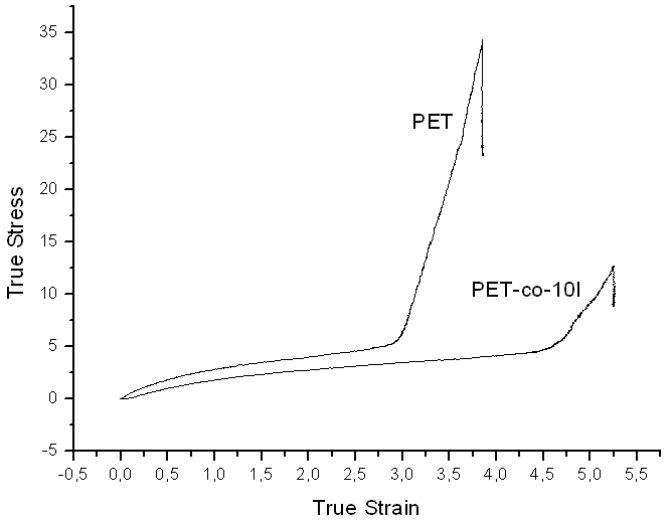

Figure 3.22- Comparison of Stress Strain curves of PET and PET-co-10I.

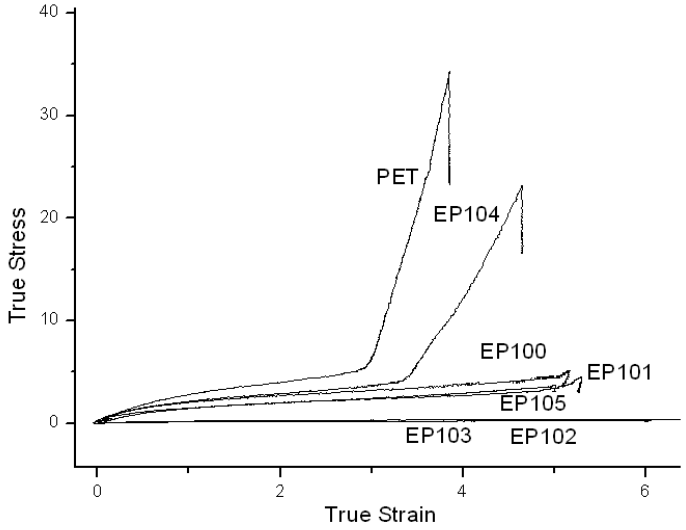

Figure 3.23- Stress strain curves of PET blends.

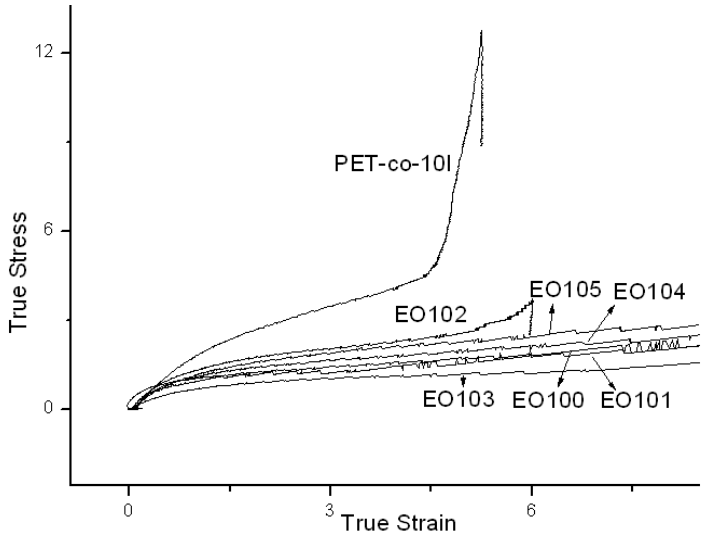

Figure 3.24- Stress strain curves of PET-co-10I blends.

CHAPTER 4

4. CONCLUSION

This study aimed to analyze and understand various factors and their relationships affecting barrier properties of PET/N-MXD6 blends. Due to lack of extensive studies in PET/N-MXD6 blends the knowledge gained in this thesis is extremely important. Most of the studies focused on a single topic for this blends like strain induced crystallization [37], copolymers[20], compatibilization [34], color generation [7] and barrier properties [4]. On the other side, this thesis project combined orientation, compatibilization, crystallinity, chemical modification by copolymers and barrier properties of PET/N-MXD6 blends.

Working conditions of extrusion and film casting were determined by DSC thermograms of the polymers used. According to that, extrusion was realized at 265ºC. Thermo gravimetric analysis showed that working temperatures for both extrusion and film casting were far below from decomposition temperatures (375-433 ºC). Changes in molecular weight of blends were analyzed with a Cannon Fenske Viscometer. Intrinsic viscosity (IV) values of the blends were above 0,65 dL/g which is the minimum necessary IV for producing high quality films. During extrusion, hopper is purged with nitrogen and closed with a PE sheet to avoid hydrolytic degradation of PET.

Particle size distribution of the dispersed phase of the blends showed significant differences depending on the matrix phase (PET or PET-co-10I), compatibilizer type and combinations used. N-MXD6 had a particle size of 2 μm in average in uncompatibilized blends for PET matrix, while using PET-co-10I which contains 10 wt.% isophthalic acid decreased particle size to 0,3 μm. Carboxyl (-COOH) group in isophthalic acid and methylene ($-CH_2$) group in N-MXD6 binds to the benzene ring in meta position. Therefore meta-phenylene linkage that both N-MXD6 and PET-co-10I have resulted in better compatibility when compared to the PET/N-MXD6 blend. The smallest particle size (0,1 μm for PET blends, 0,15 μm for PET-co-10I blends) has been observed for blends when used PET-co-5SIPA as the compatibilizer. HTPB and CTPB also reduced particle size of the N-MXD6 due to their functional groups; however the strong interaction between PET-co-5SIPA and polymers resulted in better compatibility. The efficiency of PET-co-SIPA has also been proved with the single melting peaks due to provided compatibility in DSC thermograms of blends.

Factors affecting barrier properties of the blends have been analyzed after performing gas permeability tests for each blend before and after stretching. Laminar morphology is obtained after 2x biaxial stretching which gave out an average aspect ratio of 6 for N-MXD6 nano-ellipsoids. Both oxygen and water vapor permeability reduced with the transformation of spheres into nano-ellipsoids creating a tortuous pathway for gas ingress. However, 3x biaxial stretched films resulted in high permeability which is thought to be the result of microvoids formed during stretching. Chemical modification of PET by incorporating 10 wt. % isophthalic acid in place of terephthalic acid resulted in low permeability for unstretched blends. Meta-phenylene linkage that both N-MXD6 and PET-co-10I have increases their compatibility and thus barrier properties. However, after stretching permeability values of the PET-co-10I blends were higher than the PET blends due to crystallization surpassing the effect of chemical compatibilization.

Crystallinity of blends has been examined by using different characterization tools like DSC and a custom made spectral-birefringence stretcher. Permeability of PET films decreased with crystallization induced during stretching. However, no common trend has been observed for all the films studied due to meta linkages of N-MXD6 and PET-co-10I hindering crystallization. Crystallization decreased the cold crystallization

temperature of the blends and decreased the area of the cold crystallization peak. A typical strain induced crystallization behavior of PET was observed with the birefringence vs. true stress plots. PET-co-10I and blends showed retardation in strain hardening of the films due to their meta linkages hindering crystallinity which is not favored in industrial applications.

The lowest oxygen permeability values obtained are 0,114 ml.cm/m^2.day for EP102 film stretched biaxially 2x and 0,130 ml.cm/m^2.day for unoriented EO103 film. The lowest water vapor permeability values obtained are 0,078 for PET film stretched biaxially 3x and 0,102 for unoriented PET-co-10I film. The results revealed that stretching ameliorates the barrier properties of PET films due to strain induced crystallization and tortuosity factor. On the other hand stretching affects barrier properties of PET-co-10I blends negatively. The compatibilization of PET-co-10I and N-MXD6 provides low permeability values without stretching. However, as stretching and orientation is used to provide uniformity in thickness and properties of the films extensively in polyester processing, PET-co-10I blends are not industrially applicable.

CHAPTER 5

5. FUTURE WORK

In order to provide further improvement of the barrier properties of PET/N-MXD6 blends, future studies that are crucially important will be listed in this section.

- Data that have been collected in this thesis are single readings due to lack of time and biaxial stretcher. Laboratory films can be quite variable with gels and nonuniformity. Therefore in future several samples from each film will be analyzed and statistical distribution of the properties will be checked. Response surface models will be created with the application of analysis of variance (ANOVA) that would make it possible to observe the effect of different parameters on permeability. Thus it will be possible to find the optimum conditions for high barrier properties.

- CTPB and HTPB are used as compatibilizers. Their active barrier properties resulting from their double bonds will be analyzed in future. FTIR or other spectroscopy methods could be applied to investigate the existence of double bonds after extrusion which provides active barrier properties.

- Strain rate of 1mm/sec is used for biaxial stretching and 20 mm/sec is used for uniaxial stretching. The optimization of strain rate will be performed for each blend in order to reach optimum properties.

- Draw temperature is chosen to be in between Tg and onset of Tcc. 90 ºC was applied as draw temperature in this thesis. Draw ratio is chosen to be 2 and 3. The effects of different draw temperatures and draw ratio will be analyzed.

- Tortuosity factor which is the ratio of distance travelled by oxygen to the film thickness is an important factor affecting barrier properties. The tortuosity factors of each film after stretching will be obtained. It could be obtained by measuring the distance travelled by the gas with the help of an SEM image as shown in Figure 4.1 showing the film embedded in an acrylic resin. The thickness of the film is measured to be 31,44 µm. Also other possible methods to obtain tortuosity factor will be investigated.

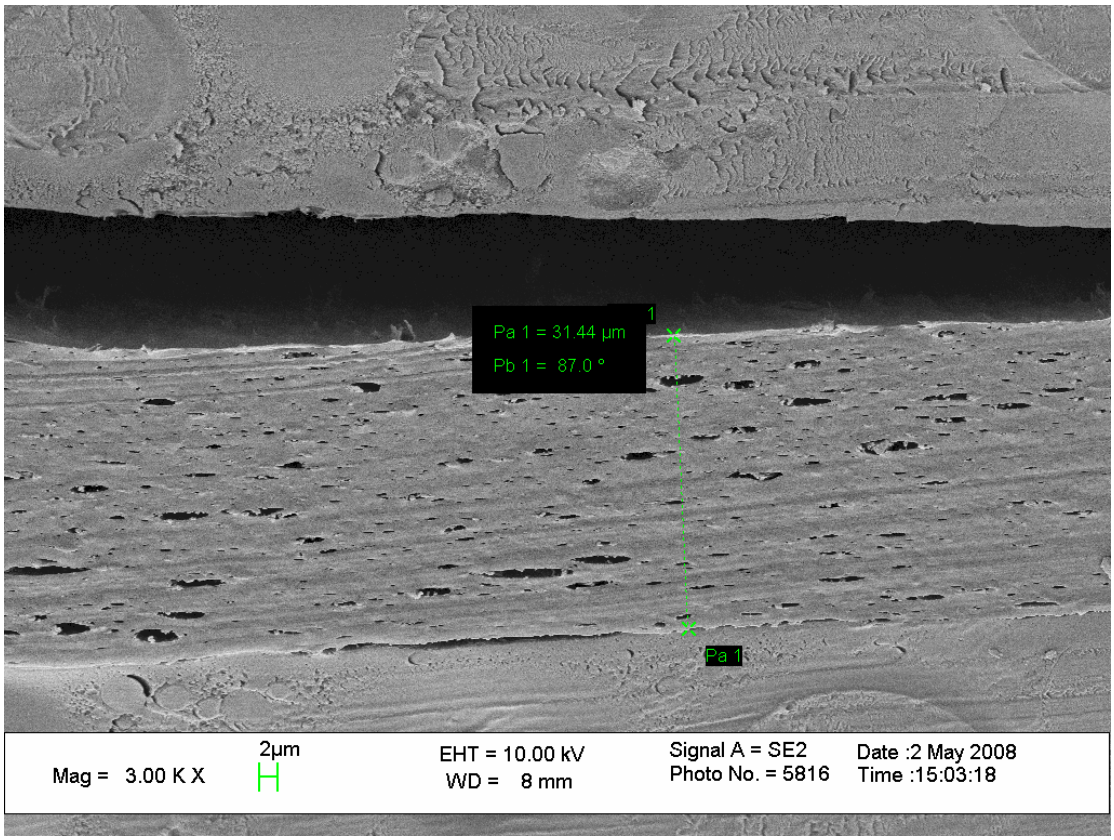

Figure 5.1- SEM image of a biaxially stretched film showing dispersed nano-ellipsoids.

- The effect of percentage of N-MXD6 on tortuosity factor will also be examined. Only 5 % N-MXD6 has been used in this thesis. However, as a further study different blends with different contents of N-MXD6 will be prepared and their effect on permeability and tortuosity factor will be investigated.

- Processing parameters and machine properties also have an effect on final film properties. It could be possible to obtain low particle size without adding compatibilizers by changing screw design, screw speed and processing temperature.

- It is very well known that conditioning the films before stretching facilitates drawing of the dispersed phase to a high aspect ratio during orientation [4]. However in this thesis the films were stretched without conditioning. As future studies the conditioning of the films should be done and resulting morphology with higher aspect ratio and barrier properties should be investigated.

REFERENCES

1. Harper, C.A., *Handbook Of Plastics, Elastomers & Composites*. 4 Ed. 2002, New York: Mcgraw-Hill Professional.

2. *Türkiye'de Plastik Endüstrisine Bakiş*. [Cited; Available From: www.tspmakine.com/egitim/file/turkiyede_plastik.pdf.

3. Samios, C.K., Kalfoglou, N. K. , *Compatibilization Of Poly(Ethylene-Co-Vinyl Alcohol) (Evoh) And Evoh/Hdpe Blends With Ionomers. Structure And Properties.* . Polymer 1998. 39(16): P. 3863-3870.

4. Hu, Y.S., Prattipati, V., Mehta, S., Schiraldi, D.A., Hiltner, A., Baer, E., , *Improving Gas Barrier Of Pet By Blending With Aromatic Polyamides.* Polymer, 2005. 46: P. 2685-2698

5. [Cited; Available From: http://www.gasbarriertechnologies.com/mxd6.html.

6. Hernandez, R.J., *Plastics Packaging- Properties, Processing, Applications, And Regulations.* . 2 Ed. 2004, Munich: Hanser Publishers.

7. Bandi, S., Mehta, S., Schiraldi, D. A., *The Mechanism Of Color Generation In Poly(Ethylene Terephthalate)/Polyamide Blends.* Polymer Degradation And Stability, 2005. 88 P. 341-348.

8. *Valor® Barrier Resins*. [Cited; Available From: http://www.valsparglobal.com/packaging/pdf/valorbarrierresins.pdf.

9. Vieth, W.R., *Diffusion In And Through Polymers*. 1991, Munich: Hanser Publishers.

10. *Two Different Test Methods: Differential-Pressure Method And Equal-Pressure Method*. [Cited; Available From: http://labthink.cn/service/show765.html.

11. Comyn, J., *Polymer Permeability*. 1985, London: Chapman & Hall.

12. *The Advantage Of Water Vapor Permeability Instrument Of Sensor Method*. [Cited; Available From: http://www.labthink.cn/service/show593.html.

13. Legaron, J.M., Catala, R., Gavara, R., *Structural Characteristics Defining High Barrier Properties In Polymeric Materials.* Mat. Sci. & Tech. , 2004. 20(1).

14. Schiraldi, D.A., Gould, S. A. C., Occelli, M. L. , *Surface Of Poly(Ethylene Terephthalate/Isophthalate) Copolyesters Studied By Atomic Force Microscopy* Journal Of Applied Polymer Science, 2001. 80 P. 750-762

15. Karayannidis, G.P., Sideridou, I. D., Zamboulis, D. N., Bikiaris, D. N., *Thermal Behavior And Tensile Properties Of Poly(Ethylene Terephthalate-Co-Ethylene Isophthalate).* . Journal Of Applied Polymer Science, 2000. 78 P. 200-207.

16. Karayannidis, G.P., Bikiaris, D. N., Papageorgiou, G. Z., Pastras, S.V. , *Synthesis And Characterization Of Poly(Ethylene Terephthalate-Co-Isophthalate)S With Low Content Of Isophthalate Units.* . Journal Of Applied Polymer Science, 2002. 86 P. 1931-1941.

17. Yu, J., Li, B., Lee, S., Ree, M. , *Relationship Between Physical Properties And Chemical Structures Of Poly(Ethylene Terephthalate-Co-Ethylene Isophthalate).* . Journal Of Applied Polymer Science, 1999. 73 P. 1191-1195.

18. Liu, R.Y.F., Hu, Y. S., Hibbs, M. R., Collard, D. M., Schiraldi, D. A., Hiltner, A., Baer, E. , *Improving Oxygen Barrier Properties Of Poly(Ethylene Terephthalate) By Incorporating Isophthalate. I. Effect Of Orientation* Journal Of Applied Polymer Science, 2005. 98: P. 1615-1628

19. Hu, Y.S., Hiltner, A., Baer, E. , *Improving Oxygen Barrier Properties Of Poly(Ethyleneterephthalate) By Incorporating Isophthalate. Ii. Effect Of Crystallization.* Journal Of Applied Polymer Science, 2005. 98: P. 1629-1642

20. Hu, Y.S., Prattipati, V., Hiltner, A., Baer, E., Mehta, S. , *Improving Transparency Of Stretched Pet/Mxd6 Blends By Modifying Pet With Isophthalate* Polymer 2005. 46 P. 5202-5210.

21. Kotek, R., Pang, K., Schmidt, B., Tonelli, A., *Synthesis And Gas Barrier Characterization Of Poly(Ethylene Isophthalate).* Journal Of Polymer Science: Part B: Polymer Physics, 2004. 42: P. 4247–4254.

22. Kong, Y., Hay, J.N., *The Measurement Of The Crystallinity Of Polymers By Dsc.* Polymer 2002. 43(14): P. 3873-3878.

23. Liu, R.Y.F., Hu, Y.S., Schiraldi, D.A., Hiltner, A., Baer, E. , *Cyrstallinity And Oxygen Transport Properties Of Pet Bottle Walls* J. Of Appl. Poly. Sci. , 2004. 94 P. 671-677.

24. Rhee, S., White, J.L. , *Crystal Structure And Morphology Of Biaxially Oriented Polyamide 12 Films.* J. Of Poly. Sci. Part B: Polymer Physics, 2002. 40: P. 1189-1200.

25. Gerlach, C., Buckley, C.P., Jones, D.P. , *Development Of An Integrated Approach To Modelling Of Polymer Film Orientation Processes.* . Transicheme, 1998. 76.

26. Gohil, R.M., *Morphology-Permeability Relationship In Biaxially Oriented Pet Films: A Relationship Between Oxygen Permeability And Prof.* J. Of Appl. Poly. Sci. , 1993. 48 P. 1649-1664.

27. Ellis, J.W., Picot, J.J.C. , *Mechanical And Thermal Anisotropy For Uniaxially And Biaxially Drawn Pet.* . Poly. Sci. & Eng. , 2000. 40(7).

28. Cakmak, M., White, J.L., Spruiell, J.E., *Structural Characterization Of Crystallinity & Crystallite Orientation In Simultaneously Biaxially Stretched And Annealed Polyethylene Terephthalate Films.* . J. Of Poly. Eng. , 1986. 6(1-4).

29. Kit, K.M., Schultz, J.M., *Morphology And Barrier Properties Of Oriented Blends Of Poly(Ethylene Terephthalate) And Poly(Ethylene 2,6- Naphthalate) With Poly(Ethylene-Co-Vinyl Alcohol).* Poly. Eng. & Sci. , 1995. 35(8).

30. Wu, W., Wagner, M. H., Qian, Q., Pu, W., Kheirandish, S., *Morphology And Barrier Mechanism Of Biaxially Oriented Poly(Ethylene Terephthalate)/ Poly(Ethylene 2,6- Napthalate) Blends.* . J. Of Appl. Poly. Sci. , 2006. 101: P. 1309-1316.

31. Matthews, R.G., Duckett R. A., Ward I. M., Jones, D. P., *The Biaxial Drawing Behaviour Of Poly (Ethylene Terephthalate).* Polymer 1997. 38(19): P. 4795 4802.

32. *Biaxial Orientation From Pet Films*. [Cited; Available From: http://www.m-petfilm.com/europe/biaxial%20orientation.htm.

33. Yeo, J.H., Lee, C. H., Park, C., Lee, K., Nam, J., Kim, S.W. , *Rheological, Morphological, Mechanical, And Barrier Properties Of Pp/Evoh Blends.* Advances In Poly. Techn. , 2001. 20(3): P. 191-201.

34. Prattipati, V., Hu, Y.S., Bandi, S., Schiraldi, D.A., Hiltner, A., Baer, E., Mehta, S. , *Effect Of Compatibilization On The Oxygen-Barrier Properties Of Poly(Ethylene Terephthalate)/Poly(M-Xylylene Adipamide) Blends.* J. Of Appl. Polym. Sci., 2005. 97 P. 1361-1370

35. Lee, S., Kim, S. , *Laminar Morphology Development And Oxygen Permeability Of Ldpe/Evoh Blends.* Polymer Eng. & Sci., , 1997. 37(2): P. Pp. 463-475.

36. Faisant, J.B., Ait-Kadi, A., Bousmina, M., Deschenes, L. , *Morphology, Thermomechanical And Barrier Properties Of Polypropylene – Ethylene Vinyl Alcohol Blends.* . Polymer . 1998. 39: P. 533.

37. Doudou, B.B., Dargent, E., Grenet, J., *Relationship Between Draw Ratio And Strain-Induced Crystallinity In Uniaxially Hot-Drawn Pet-Mxd6 Films* Journal Of Plastic Film And Sheeting, 2005. 21: P. 233-251.

38. Chandran. P., J., S., *Biaxial Orientation Of Poly(Ethylene Terephthalate). Part Ii: The Strain-Hardening Parameter.* Advances In Poly. Techn., 1993. 12(2): P. 133-151.

39. Molding Of Pet Containers, T.R. [Cited; Available From: http://www.rivapet.com/pet-containers.asp.

40. White, J.L., Cakmak, M., *Orientation.* , In *Encyclopedia Of Polymer Science And Engineering*. 1987. P. 595-618.

41. Lange, J., Wyser, Y. , *Recent Innovations In Barrier Technologies For Plastic Packaging.* . Packag. Technol. Sci. , 2003. 16: P. 149-158.

42. Lange, J., Stenroos, E., Malmström, E., Johansson, M., *Barrier Coatings For Flexible Packaging Based On Hyperbranched Polyester Resins.* Polymer, 2001. 42.

43. Lange, J., Nicolas, B., Galy, J., Gerard, J., *Influence Of Structure And Chemical Composition On Oxygen Barrier Properties Of Crosslinked Epoxy-Amine Coatings.* Polymer 2002. 43: P. 5985.

44. Jahromi, S., Moosheimer, U. , *Oxygen Barrier Coatings Based On Supramolecular Assembly Of Melamine.* Macromolecules, 2000. 33: P. 7582.

45. *Coca-Cola's Barrier Technology To Double Pet Shelf-Life.* Packaging World 1999: P. 2.

46. Garbassi, F., Occhiello, E. , *Plasma Deposition Of Silicon-Containing Layers On Polymer Substrates.* Macromol. Symp. , 1999. 139: P. 107.

47. Erlat, A.G., Spontak, R.J. ,Clarke, R.P. Et Al. , *Siox Gas Barrier Coatings On Polymer Substrates: Morphology And Gas Transport Considerations.* J. Phys. Chem. , 1999. 103: P. 6047.

48. Flodberg, G., Hellman, A., Hedenqvist, M., Sadiku, E., Gedde, U. W. , *Barrier Properties Of Blends Based On Liquid Crystalline Polymers And Polyethylene.* Polym. Sci. Eng., 2000. 40: P. 1969.

49. Scherb, P., *New Barrier Technologies For Pet Bottles.* Drink Technol. Marketing 2000. 32.

50. Brennan, D.J., Silvis, H.C., White, J.E., Brown, C.N., *Amorphous Phenoxy Thermoplastics With An Extraordinary Barrier To Oxygen.* Macromolecules 1995. 28: P. 6694.

51. *Ticona Product Information. Vectran Liquid Crystalline Polymer. Exceptional Barrier Packaging Resins For Conventional Film-Converting Equipment. Ticona Celanese Ag, Frankfurt Am Main, Germany* 2000.

52. Pinnavaia, T.J., Beall, G.W. , *Polymer-Clay Nanocomposites.* . 2000, Chichester: Wiley.

53. Gusev, A.A., Lusti, H. R. , *Rational Design Of Nanocomposites For Barrier Applications.* . Adv. Mater. , 2001. 21: P. 13.

54. Fredrickson, G.H., Bicerano, J. , *Barrier Properties Of Oriented Disc Composites.* J. Chem. Phys. , 1999. 110: P. 2181.

55. Dumont, M.J., Valencia, A. R., Emond, J. P., Bousmina, M. , *Barrier Properties Of Polypropylene/ Organoclay Nanocomposites.* J. Appl. Poly. Sci. , 2007. 103: P. 618-625.

56. Solovyov, S.E., Goldman, A. Y. , *Optimized Design Of Multilayer Barrier Films Incorporating A Reactive Layer. I. Methodology Of Oxygen Ingress* Journal Of Applied Polymer Science 2006. 100(3): P. 1940-1951.

57. Jakobsen, M., Risbo, J. , *A Simple Model For The Interaction Between Water Vapour And Oxygen Transmission In Multilayer Barrier Materials Intended For Food Packaging Applications* Packag. Technol. Sci. , 2007.

58. Citterio, C., Selli, E., Testa, G., Bonfatti, A.M., Seves, A. , *Physico-Chemical Characterisation Of Compatibilized Poly(Propylene)/Aromatic Polyamide Blends.* Angew. Makromol. Chemie 1999. 270(22).

59. Nir, Y., Narkis, M., Siegmann, A. , *Permeation Through Strongly Interacting Polymer Blends: Evoh/ Copolyamide-6/6.* Polym. Networks Blends 1997. 9(7): P. 139.

60. De Petris, S., Laurienzo, P., Malinconico, M., Pracella, M., Zendron, M. , *Study Of Blends Of Nylon 6 With Evoh And Carboxyl-Modified Evoh And A Preliminary Approach To Films For Packaging Applications.* J. Appl. Polym. Sci. , 1998. 68 P. 637.

61. Datta, S., Lohse, D. J., *Polymeric Compatibilizers. Uses And Benefits In Polymer Blends*. 1996, Munich: Hanser. 6-59.

62. Iyer, S., Schiraldi, D. A. , *Role Of Ionic Interactions In The Compatibility Of Polyester Ionomers With Poly(Ethylene Terephthalate) And Nylon 6.* . J. Of Poly. Sci. Part B: Polymer Physics, 2006. 44: P. 2091-2103.

63. Gemeinhardt, G.C., Moore, A. A., Moore, R. B. , *Influence Of Ionomeric Compatibilizers On The Morphology And Properties Of Amorphous Polyester/Polyamide Blends.* . Poly. Eng. & Sci., 2004. 44(9): P. 1721- 1731.

64. Boykin, T.L., Moore, R. B. , *The Role Of Specific Interactions And Transreactions On The Compatibility Of Polyester Ionomers With Poly(Ethylene Terephthalate) And Nylon 6,6.* Poly. Eng. & Sci., 1998. 38(10): P. 1658-1665.

65. *Polyester*. [Cited; Available From: http://www.hififilm.com/what_is_polyester.html.

66. *Polyethylene Terephthalate*. [Cited; Available From: http://en.wikipedia.org/wiki/polyethylene_terephthalate.

67. Valladares, D., Yalcin, B., Cakmak, M. , *Long Time Evolution Of Structural Hierarchy In Uniaxially Stretched And Retracted Cross-Linked Natural Rubber.* Macromolecules 2005. 38: P. 9229-9242.

68. Chandran. P., J., S., *Biaxial Orientation Of Poly(Ethylene Terephthalate). Part 1: Nature Of The Stress - Strain Curves.* Advances In Poly. Techn., 1993. 12(2): P. 119-132.

APPENDIX A. MASS TRANSFER IN POLYMERIC MATERIALS

Diffusion coefficient, D, is a kinetic property, describing the movement of permeant through a polymer. Fick's first law in one dimension defines diffusion coefficient as:

$$F = -D\frac{\partial c}{\partial x} \qquad \text{(A.1)}$$

The solubility coefficient, S, is a thermodynamic property, that decribes the dissolution of permeant in a polymer. The solubility coefficient is defined in Henry's law of solubility as:

$$C = Sp \qquad \text{(A.2)}$$

Permeability coefficient P is derived from Henry's law of solubility applied to Fick's law diffusion:

$$F = \frac{q}{At} = -D\frac{\partial c}{\partial x} = -D\frac{c2 - c1}{l} = DS\frac{p2 - p1}{l} = DS\frac{\Delta p}{l}$$

$$P = DS = \frac{ql}{At\Delta p} \qquad \text{(A.3)}$$

where F is the permenant flux, q is the heat quantity, A is the cross sectional area, t is the time, c is the concentration, x is the direction of mass transport, p is the pressure and l is the thickness [56].

APPENDIX B. CALCULATION OF GAS TRANSMISSION RATE

Differential Pressure Mehtod

Through the following formula (offered by ISO 15105-1) , gas transmission rate (GTR) can be calculated with a high precision vacuum gauge. The result unit is $cm^3/m^2 \cdot 24h \cdot 0.1Mpa$.

$$GTR = \frac{V_c}{RxTxp_uxA} x \frac{dp}{dt} \qquad \text{(B.1)}$$

V_c : volume of low-pressure side

T : test temperature

A: effective transmission area

dp/dt : pressure variation on low pressure side per unit time after the transmission becomes stable

R: gas constant.

Equal Pressure Method

The commonly used measuring unit is $cm^3/m^2 \cdot d$. Calculating formula of OTR offered by the standard ISO 15105-2 is that

$$OTR = \frac{k(U - U_o)}{A} x \frac{p_a}{p_0} \qquad \text{(B.2)}$$

U: output signal of zero voltage in testing.

U_0 :is the signal for zero voltage.

P_a : environment atmospheric pressure

P_0: : oxygen partial pressure in testing gas.

A :effective transmission area.

APPENDIX C. OTR AND WVTR VALUES OF THE FILMS

as cast	OTR(ml/m2.d)	Thickness(mm)	WTR(g/m2.24h)	Thickness(mm)
PET	21,580	0,180	12,786	0,197
EP100	40,180	0,105	13,882	0,122
EP101	30,910	0,105	11,755	0,128
EP102	17,830	0,167	6,018	0,2107
EP103	15,290	0,176	6,018	0,2052
EP104	14,910	0,172	9,563	0,176
EP105	19,310	0,152	6,791	0,2005
PET-co-10I	16,700	0,213	5,309	0,2052
EO100	32,610	0,090	17,476	0,2176
EO101	10,140	0,230	4,084	0,2923
EO102	8,010	0,222	5,357	0,2069
EO103	6,310	0,206	4,760	0,2313
EO104	8,090	0,202	5,212	0,2187
EO105	10,930	0,181	5,663	0,208
2x	OTR(ml/m2.d)	Thickness(mm)	WTR(g/m2.24h)	Thickness(mm)
PET	182,210	0,030	25,114	0,042
EP100	261,200	0,010	66,822	0,025
EP101	119,860	0,010	17,750	0,068
EP102	67,200	0,017	29,498	0,056
EP103	90,480	0,014	26,162	0,052
EP104	106,990	0,019	27,274	0,055
EP105	109,950	0,016	25,518	0,059
PET-co-10I	84,690	0,040	48,595	0,054
EO100	149,520	0,012	26,517	0,041
EO101	52,740	0,030	25,630	0,072
EO102	135,670	0,014	20,296	0,068
EO103	191,400	0,010	15,074	0,072
EO104	65,780	0,043	22,262	0,064
EO105	78,000	0,018	30,852	0,063
3x	OTR(ml/m2.d)	Thickness(mm)	WTR(g/m2.24h)	Thickness(mm)
PET	272,300	0,018	47,854	0,016
EP100	379,340	0,013	97,010	0,038
EP101	63,340	0,020	51,399	0,019
EP102	180,590	0,014	51,866	0,038
EP103	255,260	0,011	67,659	0,030
EP104	181,130	0,018	49,820	0,037
EP105	278,100	0,017	92,751	0,031
PET-co-10I	277,790	0,026	25,276	0,038
EO100	150,160	0,025	28,434	0,045
EO101	150,240	0,020	22,536	0,041
EO102	156,960	0,021	51,045	0,025
EO103	274,170	0,013	42,551	0,062
EO104	131,950	0,037	36,153	0,050
EO105	194,240	0,032	60,005	0,031